Impact of Hidden Node Problem in Association and Data Transmission for LAA Wi-Fi Coexistence

Vanlin Sathya[+], Muhammad Iqbal Rochman[+], Thomas Valerian Pasca[•], and Monisha Ghosh[&]

[•]*Indian Institute of Technology Hyderabad, India*
[+]*Department of Computer Science, University of Chicago, Illinois, USA.*
[&]*Deparment of Electrical Engineering, University of Notre Dame, USA*

Abstract

Small-cell LTE and Wi-Fi networks has been globally deployed in the unlicensed 5 GHz bands, leading to the need for new coexistence regulations between two very different access technologies. To address coexistence challenges, 3GPP standardized LTE Licensed Assisted Access (LAA) in 5 GHz bands through the incorporation of similar sensing and back-off features. The success of LAA's fair and efficient coexistence with Wi-Fi can be considered a benchmark for collaborative cellular operation in unlicensed bands. In this paper, we discuss the hidden node scenario when T-Mobile LAA coexists with the Wi-Fi APs that we deployed at the Illinois Institute of Technology (IIT) university campus. In this setup, we observed problems on the Wi-Fi client association and inefficient data transmission when it tries to connect to its corresponding Wi-Fi APs. As LAA is unaware of the Wi-Fi AP's transmission (low transmission power received at LAA BS), LAA BS continuously transmits with maximum transmission opportunity time, thus highly impacting Wi-Fi performance. Further, the hidden node problem is modeled analytically capturing the root cause of inefficiency.

1. Introduction

5G LTE, which operates in the licensed band, and IEEE 802.11 wireless LAN (Wi-Fi), which operates in an unlicensed band, have some fundamental differences in its structure. For instance, in LTE, spectrum control is centralized, *i.e.,*a base station (BS) exclusively allocates the radio resources to the connected users. Thus, there is no possibility of interference due to concurrent transmission by the users. On the other hand, Wi-Fi follows a distributed approach where each user independently contests to occupy the channel, since convergent transmission results in interference. The main motive for LTE/Wi-Fi coexistence is the use of unlicensed bands for LTE users as well as Wi-Fi users. Thus, the studies on the coexistence of LTE/Wi-Fi mainly focus on intelligent and fair use of the unlicensed band by the LTE users and keeping the incumbent Wi-Fi users unaffected.

There are two variants of unlicensed spectrum usage in LTE *i.e.,* LTE-Unlicensed (LTE-U) proposed by the LTE-U forum and the more dominant Licensed Assisted Access (LAA) standard proposed by 3GPP. The LTE-U [1] employs duty cycle access *i.e.,* ON and OFF mechanism. In numerous circumstances, LTE-U/Wi-Fi coexistence performs poorly [3]. The reasons are manifold, although two are prominent: a) LTE-U's duty-cycle mechanism often initiates LTE transmissions during active Wi-Fi transmissions, causing co-channel interference, lowering data rates, and increasing transmission errors, and b) the carrier sense mechanisms of LTE-U and Wi-Fi are inherently asymmetric [4]. On the other hand, LAA [2] follows a carrier-sensing approach called Listen Before Talk (LBT), which is similar to Wi-Fi. While the LBT access mechanism is not mandatory in the US, it is necessary in the rest of the world. As a

[1]Email: vanlins8@gmail.com (Vanlin Sathya)

result, the adoption of LTE-U by carriers has been minimal thus far, and 3GPP-standardized LAA is the predominant coexistence mechanism in practice and will be our primary focus in this work too.

In our previous research [4, 5, 6], we have focused our observation on both LAA and LTE-U mechanisms in real-time, which shows adverse affects to the Wi-Fi users and were ignored by the existing literature. Some of the observations are: a) static channel allocation to LAA node/BS in an unlicensed band, b) difficulty in association to the Wi-Fi access point (AP) by the Wi-Fi users due to high duty cycle (*i.e.,* repeating ON and OFF intervals in the medium) in LTE-U, c) a considerable reduction in the duration of duty cycle in LTE-U if several surrounded Wi-Fi APs are also considered in the estimation.

The coexistence of Wi-Fi and LAA leads to many research challenges, such as optimizing the energy detection threshold of LAA [7], dynamic adjustment of contention window size for fair sharing [8], resource allocation, and interference management [10]. These existing researches are mostly in analysis and simulation. More recently, we observed more dense LAA nodes deployed by the cellular operator based on 3GPP Release-13 *i.e.,* the downlink transmission is in the unlicensed spectrum, and the uplink transmission is in the licensed spectrum. Thus, there is a need to study the LAA and Wi-Fi coexistence of various US carrier operators (such as T-Mobile, AT&T, and Verizon) in real-time. An Android APP developed in the University of Chicago, namely SigCap[2], was used to collect real-time data such as Channel Assignment, Bandwidth, Reference Signal Received Power (RSRP), Reference Signal Received Quality (RSRQ), and Received Signal Strength Indicator (RSSI) from various LAA nodes deployed by operators in downtown Chicago. This data is freely available for academic and industry researchers [11]. In our previous work [12], we presented such measurements from various locations in Chicago, where the carriers deployed LAA networks close to Wi-Fi networks. We believe this is the first such real-world measurement campaign of LAA using end-user devices (*i.e.,*smartphones). From these measurements, we cannot perform the controlled interference experiments because we have no control over the Wi-Fi AP's parameters. These include operating bandwidth (narrow vs. broad), number of Wi-Fi clients, number of Wi-Fi APs deployed per channel, static channel allocation, and deployment location. Hence, to perform the controlled experiment, we used an experiment space at the Illinois Institute of Technology (IIT) campus (where T-Mobile LAAs were deployed) to deploy our own Wi-Fi APs and present our analysis in this paper. We observed many open coexistence problems such as LAA static channel allocation, Dynamic Transmission Opportunity (TXOP), turning OFF on LAA transmission, coexistence impact on the downlink and uplink transmission, and hidden terminal problems.

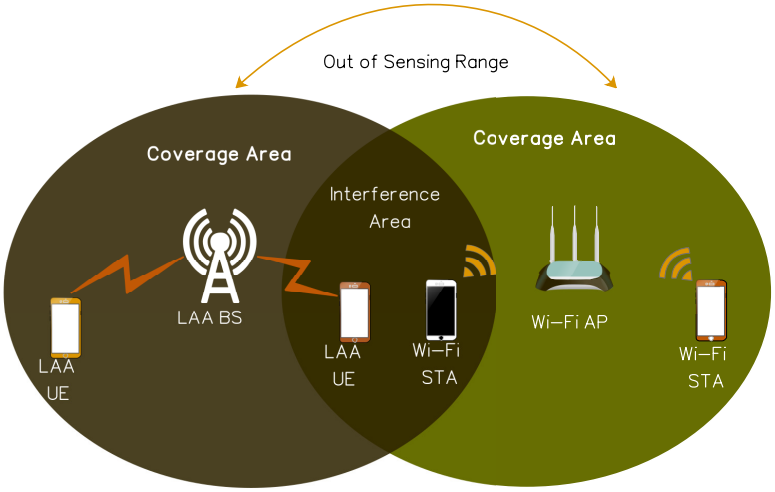

Figure 1: Hidden Node Problem in LAA Wi-Fi Coexistence.

In the legacy LTE operation, Channel Quality Index (CQI) is reported to the BS by a User Equipment (UE), and consist of a value between the range of 0 to 15, which is derived from SINR. CQI can serve as a metric for the

[2]https://people.cs.uchicago.edu/~muhiqbalcr/sigcap

interference strength on a carrier, and additionally, it is also possible to infer RSSI from RSRP and RSRQ reports. To determine hidden node at an LAA enhanced Node B (eNB), the combination of CQI, RSRP, and RSRQ data can be used, for example, by correlating the channel quality perceived by two LAA UE with the same RSRP, but one UE is affected by a hidden node problem. However, the transmission of Discovery Reference Signal (DRS) is required for the measurement of RSRP, RSRQ, and CQI, and contrary to the legacy LTE Reference Signal, it is not transmitted in a strict periodical manner in the unlicensed spectrum due to LBT. To solve this, LAA has introduced new metrics in Radio Resource Management (RRM) report, *i.e.,* average SINR, used to determine channel occupancy. The channel occupancy is the percentage of time when the average SINR is above a configured threshold. The period between measurements are {40, 80, 160, 320, 640} ms, which is longer when compared to the legacy LTE. Hence, this feedback is not instant, which is non-optimal for detecting hidden node problems.

In this work, we focus on the hidden node scenario when T-Mobile LAA coexists with our deployed Netgear Wi-Fi APs at the IIT university campus. We observed the Wi-Fi client association problem and the inefficient data transmission problem when it tries to connect to its corresponding Wi-Fi APs by capturing the Wireshark at the Wi-Fi transmission and reception side. In this setup, LAA is not entirely aware of the Wi-Fi AP transmission (due to its low receive energy power), which leads to a maximum transmission opportunity on the LAA side. Hence, most of LAA and Wi-Fi packets are collided, leading to a throughput reduction on both sides but higher reduction on the Wi-Fi side.

Further, we develop an analytical model to capture inefficiencies in the LAA and Wi-Fi coexistence. The analytical model includes the collision at hidden nodes due to LAA transmissions and compared it with the hidden node collision on a Wi-Fi and Wi-Fi coexistence. We found that there are delays due to LAA's inability to sense transmission in the Wi-Fi ambit at the hidden Wi-Fi nodes/STAs. Lastly, the throughput reduction in the case of the saturated scenario is also presented.

The paper is organized as follows. Section 2 provides a brief overview of LAA and 5 GHz coexistence, focusing on overview and challenges in hidden node scenarios and Wi-Fi client association problems. In Section 3, we discuss the LAA and Wi-Fi channel access categories. The experimental setup of the deployment studies and configurations of LTE and Wi-Fi coexistence in the IIT campus is described in Section 4. Section 5 explains the hidden node scenario, and analysis of hidden node Wi-Fi stations. Section 6 describes the real-time issues in the hidden node association process and experiment result and study in detail. Section 7 explains the validation of hidden node Wi-Fi stations. In Section 8, we have presented the conclusions and future research directions.

2. LAA and Wi-Fi Coexistence: Overview and Challenges

In this section, we summarize current studies of LAA and Wi-Fi coexistence in the unlicensed spectrum while also highlighting potential issues of coexistence.

2.1. Hidden Node Scenario and Related Works

The hidden node problem is a problem common to wireless networking in which a wireless transmitter cannot communicate to the receiver due to interference at the receiver which cannot be sensed at the transmitter. IEEE standards proposed to use of small reservation packets like Request to Send (RTS) and Clear to Send (CTS) to solve the hidden node problem in traditional Wi-Fi to Wi-Fi coexistence. In LAA and Wi-Fi coexistence, hidden node problems can happen due to the radio access difference between Wi-Fi and LAA as shown in Fig. 1, where LAA BS is not aware of the Wi-Fi STA transmission in the interference zone. There is no coordination between LAA and Wi-Fi, *i.e.,*LAA BS cannot decode Wi-Fi signals to determine transmission duration for a reliable back-off. Furthermore, the asymmetry of LAA (*i.e.,* -72 dBm) and Wi-Fi energy detection levels (Preamble: -82 dBm and data: -62 dBm) may cause Wi-Fi client's RTS packet be ignored by the BS. In [29], a hidden node problem over shared medium access networks is addressed to reduce or avoid performance degradation problems, by studying the CQI, RSRP, and RSRQ metrics on the context of LAA UEs facing different levels of interference in the hidden node scenario.

In the LTE-U/Wi-Fi coexistence, [30, 31] proposed a mechanism to address Wi-Fi performance degradation from hidden LTE-U eNB. The works aim to modify the regular CTS-to-Self frame and suggest transmissions of the modified

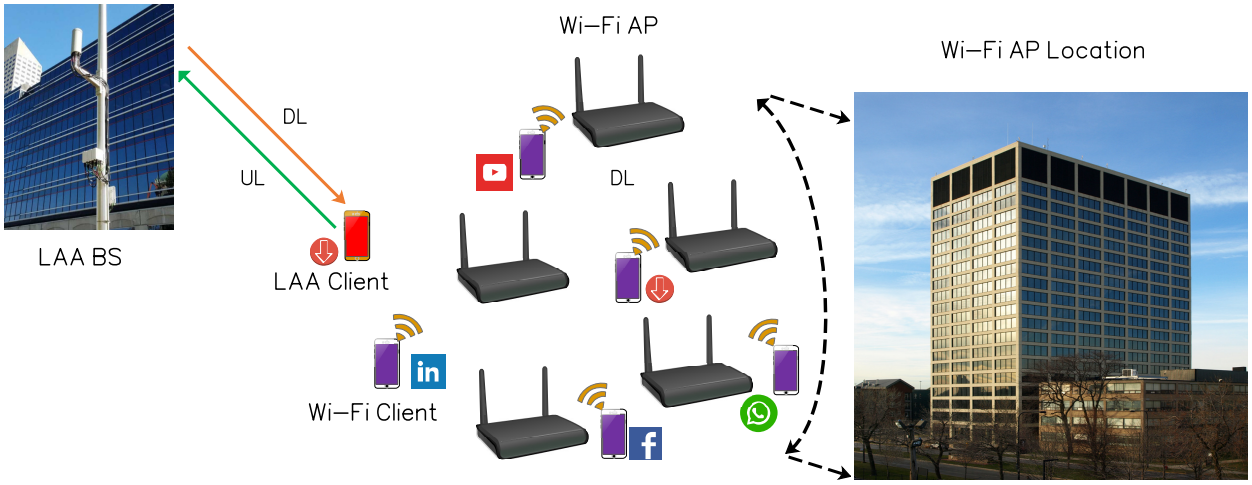

Figure 2: T-Mobile Hidden Node Experiment Scenario at IIT Campus

CTS-to-Self from LTE-U nodes to solve this hidden node issue. Furthermore, it also increased throughput by allowing simultaneous transmissions of LTE-U and Wi-Fi whenever possible. In [32], the authors argued that the immense deployment of Wi-Fi necessitates a user-oriented study to find the effects of LTE-U operation, primarily in scenarios where the LTE-U eNB remains hidden from Wi-Fi Access Point. To comprehend these effects, they performed a user-level throughput study of Wi-Fi in LTE-U's presence using a test-bed and observed unfairness in throughput distribution among Wi-Fi users. Furthermore, Wi-Fi users are disadvantaged from missing the periodic beacon frames due to LTE-U's interference.

All the realistic deployment of hidden terminal problems work on the literature discuss the LTE-U ON-OFF duty cycle coexistence with the Wi-Fi AP. There is not much work in the hidden node aspect of the LAA Wi-Fi coexistence study. In our experiment, we created a hidden node scenario where the LAA client and Wi-Fi clients are placed in the overlap region of two BS signals, as shown in Fig. 2. The Wi-Fi APs, Wi-Fi clients and LAA clients are deployed in such a way that both LAA and Wi-Fi clients can hear their respective BS and AP transmission and LAA BS can hear Wi-Fi clients and Wi-Fi AP can hear LAA UE transmission. But LAA BS and Wi-Fi AP cannot hear each other. Hence, LAA BS is unaware of Wi-Fi transmissions and proceeds, transmitting with the maximum transmission opportunity of 8 ms.

2.2. LAA and Wi-Fi Coexistence Overview and Related Works

LAA first released on 3GPP standard Release 13 [13]. In this version, the Listen Before Talk (LBT) [16][17] scheme, the operators have already implemented an energy detection threshold of -72 dBm. The LAA unlicensed operation is only enabled for downlink transmission, while all uplink and signaling are in the licensed spectrum. The standard expands with the inclusion of unlicensed uplink operation in the 3GPP Release 14, this version of LTE is called Enhanced LAA (eLAA). Moreover, Further, Enhanced LAA specifications (feLAA) are added to 3GPP Release 15 as a part of Phase 1 5G New Radio [15]. In [18], we explored the effect of energy detection (ED) threshold on Wi-Fi and LAA via extensive simulations and demonstrated that if both Wi-Fi and LTE employed a sensing threshold of -82 dBm to detect the other, overall throughput of both coexisting systems improved, leading to fair coexistence.

Since LAA requires the ED threshold to be set conservatively in the potential presence of Wi-Fi, the LAA's spatial spectrum reuse will be much impaired. Such a new limit has been introduced mainly due to ED's incapability of differentiating Wi-Fi frames from LTE frames. In [19], the author proposed a lightweight but effective Wi-Fi frame detection method with which the LAA devices can capture a Wi-Fi preamble by only using the LAA's time-domain samples while incurring minimal latency. To identify the duration of a Wi-Fi frame and dynamic ED threshold selection algorithm, the author proposed the Wi-Fi energy tracking algorithm. In [20], the author proposed an enhanced

LAA (eLAA) as a practical technique by exploiting the TXOP reservation via the Clear-to-Send-to-Self (CTS-to-Self) frame in Enhanced Distributed Channel Access (EDCA) to seamlessly integrate eLAA transmission within existing Wi-Fi protocol. To further improve throughput, the author analyzed and derived an optimized unlicensed resource allocation scheme before acquiring several intrinsic properties. The proposed coexistence framework enhances both networks' performance with a proposed simple algorithm to optimize eLAA resource access. A multi-group model was proposed [21] for LAA and Wi-Fi coexistence, as a function of respective initial back-off window sizes, sensing duration, maximum back-off stages, retry limits, and transmission opportunities. The analysis showed that LAA could maintain proportional fairness with Wi-Fi by either tuning its initial back-off window size or sensing duration. The proposed LAA parameter settings in the coexistence scenario make equal per-node airtime. In [22], the author proposed the downlink interference control scheme based on power allocation for the eNB, which protects its transmission from the interference of asymmetric hidden terminals. Through extensive simulation results, the author concludes that the proposal allows the eNB to effectively prevent the exposure boundary APs from becoming asymmetric hidden terminals.

In [23], the author proposed a time adjustment method for the load-based Equipment (LBE) mechanism to maximize the throughput of LTE while ensuring the fairness coexistence and satisfying the LTE users' data rate demands. In calculating the performance of LTE and Wi-Fi networks on an unlicensed coexistence channel, a new method considers the synchronization of BS on a licensed and unlicensed spectrum. Besides, to satisfy fairness, the author proposed a virtual Wi-Fi network construction method to deal with the situation that the Wi-Fi network offering the same level of traffic load of the LTE network does not exist on the carrier. In [24], the author derived a 3-D Markov chain model to describe the category-4 LBT procedure of an LAA eNodeB. Unlike all existing models of LTE LAA LBT procedures, this 3-D Markov model takes into account the GAP period and transmission priority in the category-4 LBT procedure, which is the significant original contribution of this work. In [25], quantitatively analyzed the Medium Access Control (MAC) delay for tagged LAA eNBs and proposed a delay-guaranteed admission control scheme. This work considered the freezing time of busy slots caused by collision or successful transmission and introduced the exponential back-off mechanism for delay analysis.

While much of the coexistence effort from industry [36, 37]is driven by fair sharing as defined by 3GPP, academic research has begun to explore coexistence fairness issues from a broader perspective, as indicated above. There are some recent work that has contributed to this issue, including ours [6, 5]. In [39] and [40], authors derived the proportional fair rate allocation approach for Wi-Fi/LAA (as well as Wi-Fi/LTE-U) coexistence. Also, [43],the fairness in the coexistence of Wi-Fi/LAA LBT based on the 3GPP criteria is investigated through a custom-built event-based system simulator. Their results suggest that LBT (and the correct choice of LBT parameters) is essential to achieving proportional fairness. In our work, we bootstrapped on the analytical model developed in [6]. We enhanced it to include the impact of different sensing duration of Wi-Fi and LAA on respective system throughput during coexistence. The proposed new analytical model results are further validated via a National Instrument (NI) test-bed. Then, we explored the issue of fair coexistence by comparing results (coexistence system operating points) from the 3GPP definition [5] to a scheme that enforces proportional fairness whereby each node in either network achieves the same fraction-of-time access. The results conclusively show that proportional fairness is a much better notion than 3GPP fairness and produces equitable results for both networks in a larger variety of scenarios.

In all the above existing literature, we discuss the issues and solutions of LAA Wi-Fi coexistence in the simulation and analysis approach. There is not much actual work on the realistic deployment of LAA and Wi-Fi coexistence study. Hence, In this work, we focus on the particular issue *i.e.,* hidden node scenario in the real-time T-Mobile LAA operator deployment in Chicago. This work gives more insight and understanding of how the coexistence in the unlicensed spectrum plays a critical impact.

2.3. Wi-Fi Client Association Problem

The Wi-Fi beacon frame is a crucial management frame. The Wi-Fi primary channel mainly used for beacon transmission and the secondary channel is used based on the demand per UE transmission. It contains all of the necessary information about the network, including AP identifier, capabilities (data rates, QoS), and BSS load. An AP periodically transmits beacon frames at a fixed time interval (typically 102.4 ms), varying from 60 to 450 bytes.

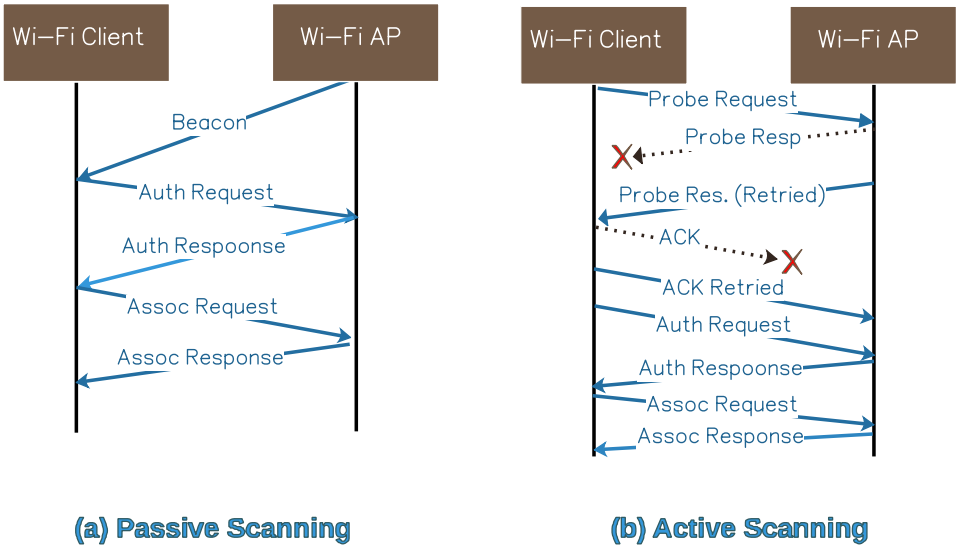

Figure 3: Wi-Fi Client Association in LAA Wi-Fi Coexistence Scenario.

There are two types of Wi-Fi scan: passive scan, where the Wi-Fi client passively listens to the beacons, and active scan, which includes an active probing by the Wi-Fi client. In the real-time deployment setup, both active and passive scanning modes supported, as shown in Fig. 3 (a) and (b). In both methods, the clients can start the association process after Wi-Fi clients received AP's beacon information. Since all packets in the association process are unicast except the beacon, it needs to be replied with ACK to complete the transmission. These unicast packets are more vulnerable to interference due to the requirement to complete ACK. Furthermore, all unicast packets need to be retransmitted on failure, thus increasing delay in the association process. Moreover, it may further be exacerbated on LAA/Wi-Fi coexistence due to interference and hidden node problem. Furthermore, Wi-Fi clients association packets may get dropped when LAA coexists with Wi-Fi AP under a hidden node scenario. This association problem is most severe when LAA BS transmits with the TXOP of 8 ms, where the Wi-Fi clients may not be able to acquire transmission opportunity to associate.

3. LAA and Wi-Fi Channel Access Categories

In this section, we discuss the different traffic access parameters and contention window features for LAA and Wi-Fi.

3.1. LAA Standard overview and Medium Access Categories

To coexist with Wi-Fi, LAA specifies an LBT mechanism implemented at the BS using an energy detection threshold of -72 dBm. However, Wi-Fi continues to use a sensing threshold of -62 dBm to defer to LAA (energy detection).

The LAA LBT channel access mechanism specifies different transmission opportunity (TXOP) times for different access categories [5]. Voice and video traffic utilize TXOPs of 2 and 3 ms, respectively, since the stringent delay requirements needed to satisfy Quality of Service (QoS) necessitate the use of short packets. However, for data, LAA specifies a maximum TXOP of 8 ms to maximize throughput. Moreover, when an LAA BS gets access to the channel, it is allowed to transmit packets for a TXOP duration of up to 10 ms if it is known a priori that there is no coexisting Wi-Fi node/STA, otherwise up to 8 ms for DL and 6 ms for UL. In most realistic traffic scenarios, such as Data, Data + Video, Data + Streaming, we observed that the LAA BS goes up to a maximum of 8 ms TXOP transmission.

Table 1: Access Categories in Downlink LAA [14]

Access Class # (DL)	**Initial CCA**	**CWmin**	**CWmax**	$TXOP$
1 (Voice)	25 μs	30 μs	70 μs	2 ms
2 (Video)	25 μs	70 μs	150 μs	3 ms
3 (Best Effort)	43 μs	150 μs	630 μs	8 ms or 10 ms
4 (Background)	79 μs	150 μs	10.23 ms	8 ms or 10 ms

Table 1 shows the details of each Access Priority Class for downlink transmission in LAA. Following an energy detection to determine if the channel is clear, the LAA BS will defer for a T_d based on the type of access category and then begin transmitting. According to the standard, a collision is detected when the Hybrid Automatic Repeat Request - Acknowledgment (HARQ-ACK) reply contains 80% Negative ACKs (NACKs). A back-off number is selected randomly from a doubled contention window size for retransmission (*i.e.*,$[0; 2^i W'_0 - 1]$, where i is the retransmission stage for selecting the contention window size). When i exceeds the maximum retransmission stage m' (the maximum window size is $W'_{m'}$), it stays at the maximum window size for e_l times (e_l is the retry limit after reaching to m') where the e_l is selected from the set of values $\{1, 2, \ldots, 8\}$; then, i resets to 0. The TXOPs assigned to the different LAA access categories shown in Table 1 are crucial to ensure fairness when coexisting with Wi-Fi.

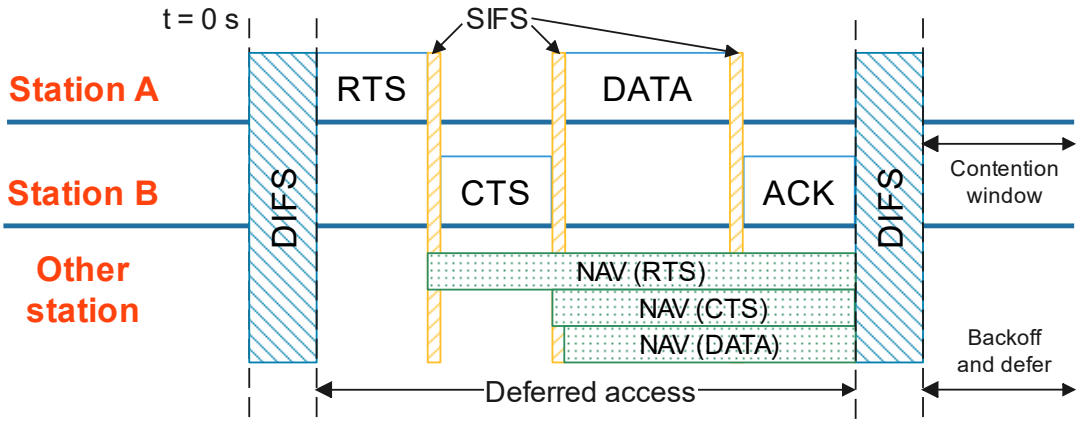

Figure 4: Wi-Fi Transmission Mechanism, CSMA/CA

3.2. Wi-Fi Mechanism and Medium Access Categories

The Wi-Fi adopts the CSMA/CA as shown in Fig. 4, which means that a station only transmits if the channel is sensed to be idle, and the station has not just completed a successful transmission. Otherwise, if the channel is busy during the DIFS sensing period or the station is contending after successful transmission, it persists with monitoring the channel until it is measured idle for a DIFS period. Then it selects a random back-off duration (counted in units of slot time) and counts down. Specifically, a station selects a back-off counter uniformly at random in the range of $[0; 2^i W_0 - 1]$ where the value of i (the back-off stage) initialized to 0 and W_0 is the minimum contention window chosen initially. Each failed transmission due to packet collision results in the back-off stage increment by 1 (binary exponential back-off or BEB), and the node counts down from the selected back-off value. If a unicast transmission is successful, the intended receiver will transmit an Acknowledgment frame (ACK) after Short Interframe Spacing (SIFS) duration post successful reception. Similar to LAA, the Wi-Fi also supports different traffic categories like background, best effort, video, and voice, as shown in Table 2. The contention window size of CWmin and CWmax for AC_BK and AC_BE is 15 and 1023 slots. The minimum CWmin for AC_VI and AC_VO is 7 and 3 slots, and the maximum CWmax for AC_VI and AC_VO is 15 and 7 slots. Due to differences in slot length, the TXOP also varies from one Wi-Fi amendments to the other.

Table 2: Access Categories in Wi-Fi 11ac

Access Category	AIFS	CWmin	CWmax	*TXOP*
Voice (AC_VO)	18 μs	27 μs	63 μs	2.08 ms
Video (AC_VI)	18 μs	62 μs	135 μs	4.096 ms
Best Effort (AC_BE)	27 μs	135 μs	9.207 ms	2.528 ms
Background (AC_BK)	63 μs	135 μs	9.207 ms	2.528 ms

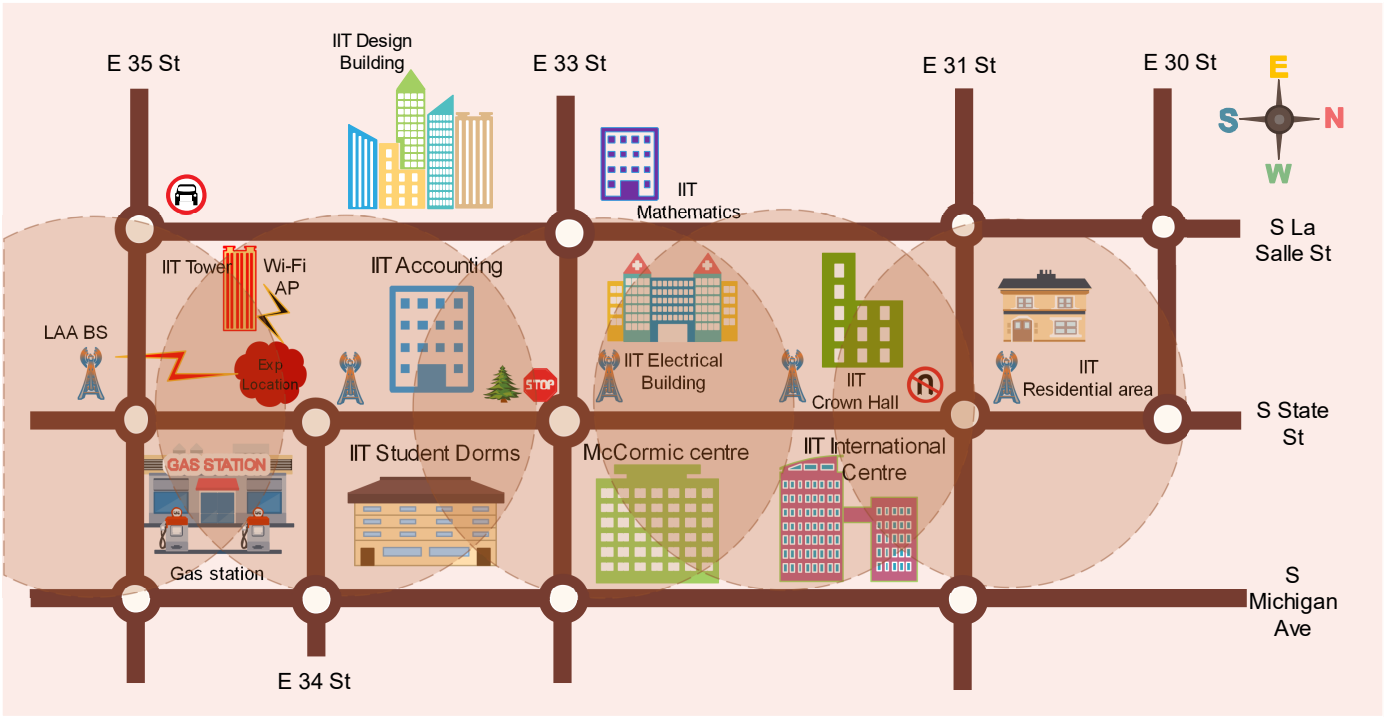

Figure 5: Experiment Location in IIT University Campus

4. Experiment Setup of the Deployment Studies on LTE and Wi-Fi Coexistence in IIT Campus

IEEE and 3GPP have worked in synchronization to achieve the agreed-upon goal of fair and efficient LTE and Wi-Fi coexistence. In this sub-section, we discuss the deployment of LAA in the IIT campus and the experiments designed to study this deployment.

4.1. Real-time Coexistence Deployments in IIT Campus

We observe the deployment of LAA based on 3GPP Release 13 by T-Mobile throughout the campus. The total number of LAA BS is 5, as shown in Fig. 2 and Fig. 5. All LAA BSs are deployed in the S. State road along the Green Line rail route, and are mounted on the lamp pole in the middle of the two way road, with the campus buildings (such as student dorms, cafeteria, Siege Hall, mechanical building, etc.) on both sides of the roads. The objective of LAA is to standardize both uplink and downlink transmissions in the unlicensed spectrum. The current pilot and commercial deployments have specifically focused on testing the downlink capabilities of LAA. The LAA deployments at this site feature a non-standalone architecture where an LTE Macro or Femtocell serve as the primary licensed carrier, with the LAA functions as an secondary carrier specifically for transmissions on the downlink.

Table 3: Hidden Node Experiment Equipment's

Parameter	Value
Ubuntu Laptop	3 (Lenovo)
Wi-Fi AP	5 (Netgear)
HUB Switch	1 (Netgear)
Wi-Fi Device Clients	5
LAA Device Client	1 (Google Pixel)
Ethernet Cable	6

The radio predominantly used in LAA deployments was Ericsson's Micro Radio 2205, which operates in the unlicensed 5 GHz band, equivalent to Wi-Fi channels 36, 40, and 44, with 20 MHz bandwidth. The deployed LAA networks have the capability of 2×2 MIMO transmissions with the maximum modulation coding scheme of 256 QAM. The operators make use of a maximum of 3 unlicensed channels, thus reaching a maximum unlicensed capacity of 60 MHz, with an additional 15 MHz provided by the primary licensed channel.

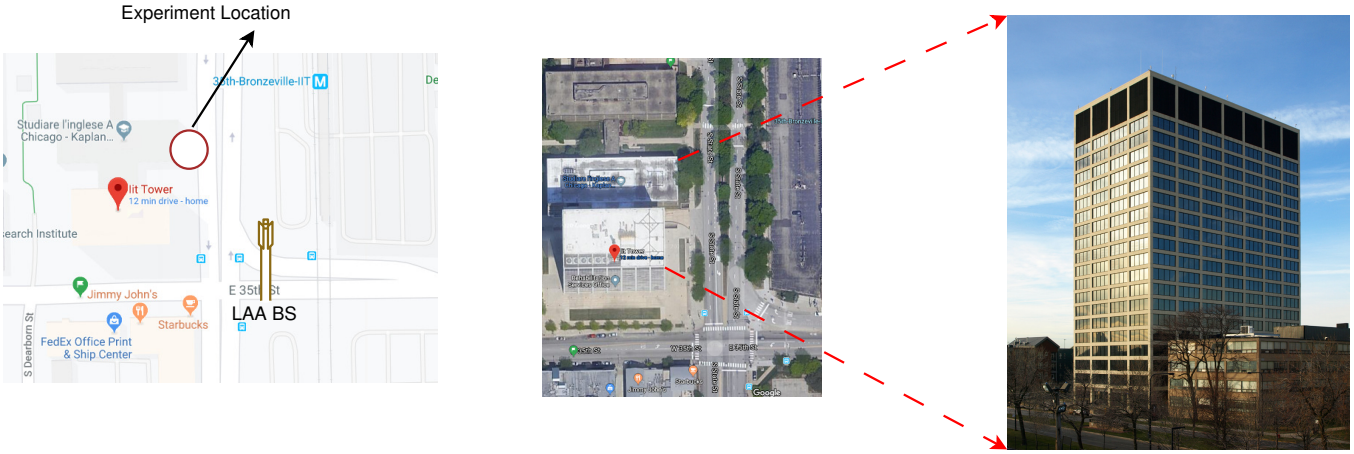

(a) Experiment & BS Location

(b) Top View: Experiment & BS Location

(c) Close View: Deployment Location

Figure 6: Experiment Location in IIT University Campus

4.2. Coexistence Experiment Setup

Fig. 6 (a) shows the location of the LAA BS and experiment site on the Google Map. Fig. 6 (b) shows the top view of the experiment location and LAA location. In general, there are numerous trees on the pathway, but as we experimented in the winter season, there were not many obstacles between LAA BS and the client, as there were no leaves on the trees. Due to this, we observed good signal penetration (typically from winter to summer, there will be signal difference [46]). Fig. 6 (c) shows the close view of the Wi-Fi AP and Wi-Fi client location. In our experiment, we deployed the Wi-Fi AP on the 3rd floor of the IIT building. We placed the LAA client on the same floor where the Wi-Fi APs are deployed and observed no LAA signal from the LAA BS. Therefore we tried to deploy the LAA client and Wi-Fi clients outside the building (on the sidewalk of the building). We also installed the Wi-Fi clients at a distance of 30 meters from the Wi-Fi APs. Hence, the Wi-Fi APs are in good Wi-Fi coverage. We placed the LAA client at a distance of 150 meters from the LAA BS. We deployed both the LAA and Wi-Fi clients at the height of 5 Feet from the ground, and the Wi-Fi AP and LAA BS are placed at the height of 40 Feet and 50 Feet, respectively. Table 3 shows the hardware equipment used in the hidden node coexistence experiment.

The Wi-Fi APs, Wi-Fi clients, and LAA clients are deployed in the hidden node scenario. The transmission power of LAA BS and Wi-Fi AP is 23 dBm, and the data traffic assumed in the experiment acts as a full buffer. Wi-Fi APs

cannot receive the LAA transmission (*i.e.,* receive power is very low that it is negligible), and similarly, LAA BS cannot receive Wi-Fi APs transmission. All Wi-Fi APs configured at the T-Mobile LAA channels, *i.e.,*36, 40, and 44. We assumed five different varieties of traffic, *i.e.,*Data, Data + Video, Live Streaming, Data + Live Streaming, and video.

- **Data (D):** Pure data traffic is generated by downloading a large YUV dataset (>10 GB) from Derf Test Media Collection [45].
- **Video (V):** A Youtube video is downloaded, with a resolution of 1920×1080 and a bit-rate of 12 Mbps.
- **Data + Video (D+V):** Combination of data and video traffic as described above.
- **Streaming (S):** A live stream video on Youtube is loaded, with a resolution of 1280×720 and a bit rate of 7.5 Mbps.
- **Data + Streaming (D+S):** Combination of data and streaming traffic as described above.

4.3. Wi-Fi AP Configuration

In our experiment, we configured five Netgear Wi-Fi AP for four different channel and bandwidth scenarios over the U-NII-1 band (5.15 to 5.25 GHz) to overlap with the LAA channels, as illustrated by Fig. 7.

1. *Fixed 20 MHz (F20):* All five Wi-Fi APs are configured on channel 36, as shown in Fig. 7 (a). In the 5 GHz spectrum, most of the Wi-Fi APs try to operate in the wider band (i.e., 40, 80 MHz). However, we still observe some resident and university campus' APs operate on 20 MHz narrow bands. Hence, we included this scenario in our coexistence experiment.
2. *Variable 20 MHz (V20):* In this scenario, we distributed the load of the Wi-Fi AP on three different 20 MHz narrow-band channels (i.e., 36, 40, 44). Because the T-Mobile LAA operates on channels 36, 40, and 44, we are trying to observe the impact of all LAA channels transmission on Wi-Fi. Hence, we configured 2 Wi-Fi AP on channel 36, 2 Wi-Fi AP on channel 40, and 1 Wi-Fi AP on channel 44, as shown in Fig. 7 (b).
3. *Varying 40 MHz (V40):* In this scenario, we configured three channels in the lower 40 MHz (5.17 to 5.21 GHz) and two channels in the upper 40 MHz (5.21 to 5.25 GHz). The breakdown for the five APs' primary channels is as follows: one primary channel in 36, two primary channels in 40, and two primary channels in 44, as shown in Fig. 7 (c).
4. *Varying 80 MHz (V80):* In this scenario, we configured all APs in the only possible 80 MHz channel in U-NII-1 (5.17 to 5.25 GHz). The primary channel assignment for the five APs is similar to V40 scenario: one primary channel in 36, two primary channels in 40, and two primary channels in 44, as shown in Fig. 7 (d).

5. Hidden Node Scenario Analysis

In this section, we explain the impact of beacon and data transmission in the hidden scenario. Finally, we discuss the analysis of the hidden Wi-Fi station in the LAA coexistence scenario.

5.1. Broadcast and Data Packet Transmission for Association Process

In this section, we discuss the different possible broadcast cases on the Wi-Fi client association process.

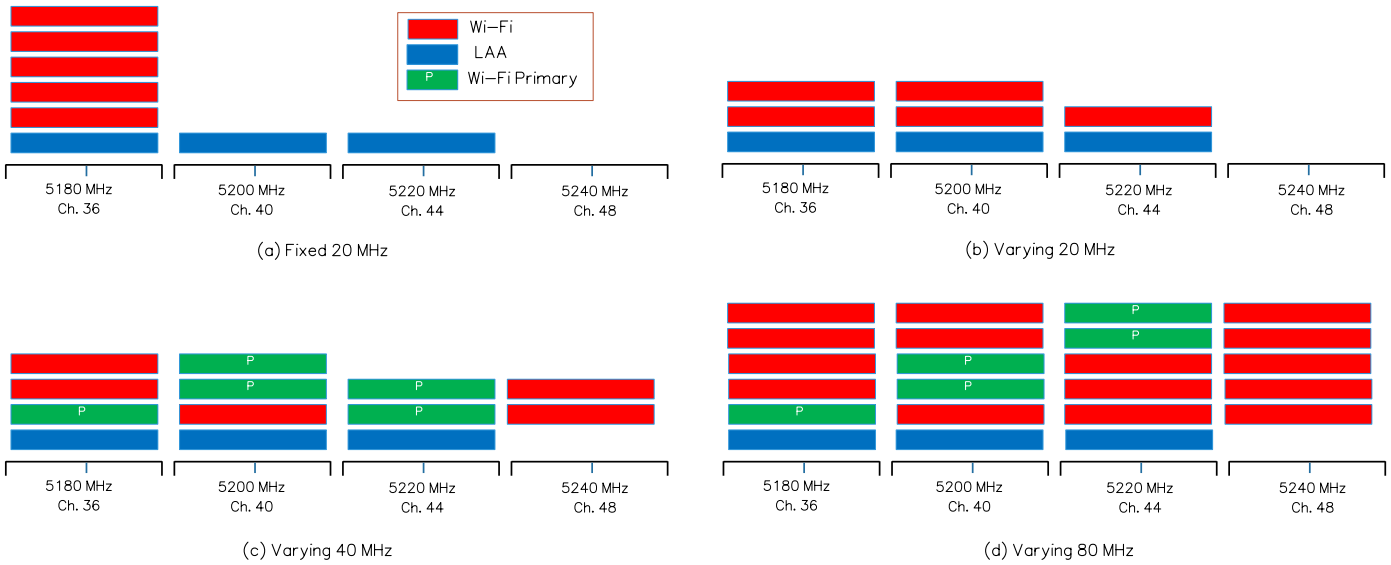

Figure 7: Wi-Fi AP Channel Configuration scenarios at IIT Campus

5.1.1. Broadcast Packet Transmission for Association and Data Process

The beacon transmission and reception in LAA and Wi-Fi coexistence are explained in three cases in this section.

Case 1 illustrates a Wi-Fi beacon transmission during the LAA transmission period. The LAA waits for Clear Channel Assessment (CCA) duration and a back-off time before occupying the channel. After waiting for a random back-off time, LAA starts its transmission. At the same time, a Wi-Fi AP operating on the same channel does beacon transmission, as shown in Fig. 8 (Case 1). The Wi-Fi AP does transmissions independent of LAA transmission because Wi-Fi AP is positioned outside the transmission range of LAA, as shown in Fig. 9. Hence the beacon received by Wi-Fi nodes/STAs, which are in the common transmission region of LAA and Wi-Fi, suffers from high co-channel interference. These beacon packets collide and do not decode successfully and leads to Wi-Fi client disassociation.

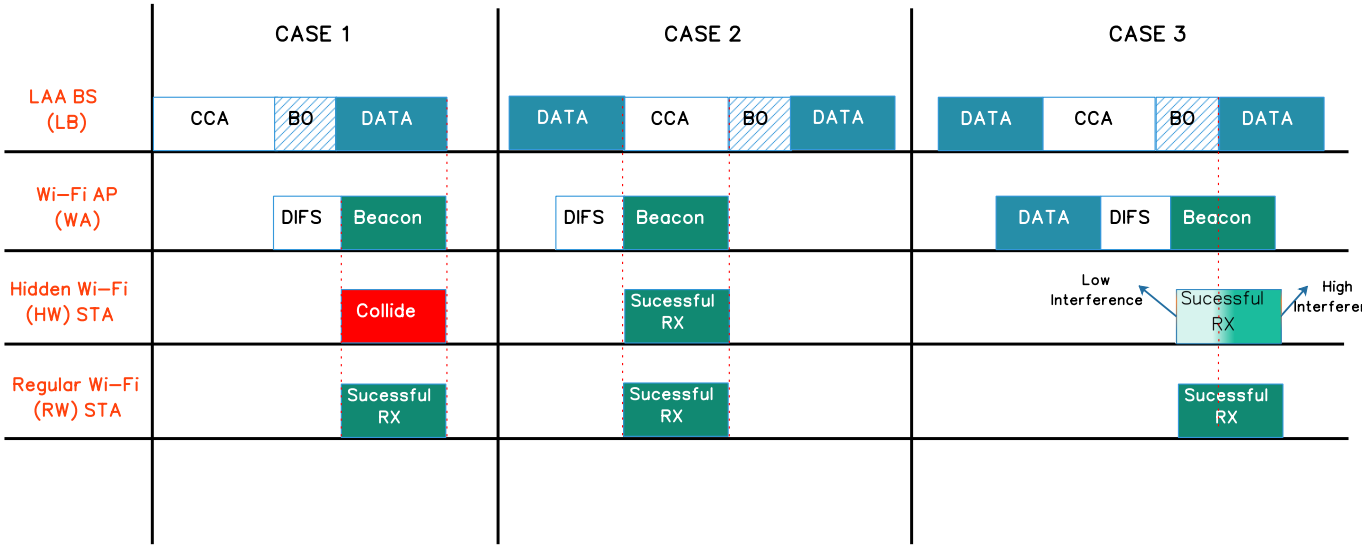

Figure 8: Wi-Fi AP Beacon Packet Transmission for Association Process

Case 2 illustrated the scenario when the Wi-Fi beacon was generated during the LAA CCA period or the LAA

transmission period, as shown in Fig. 8 (Case 2). When these packets are transmitted well within the LAA CCA period, then these Wi-Fi beacons do not suffer any collision with LAA transmissions. Hence, it leads to a successful Wi-Fi client association.

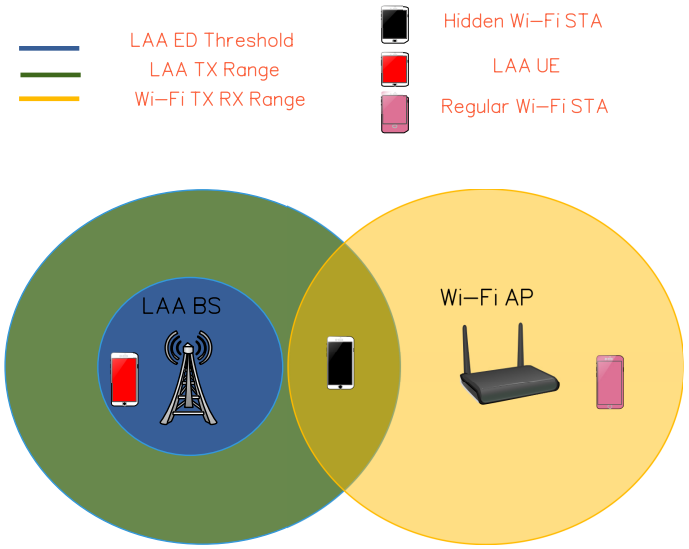

Figure 9: Simple Hidden Node Scenario for Analysis.

Case 3 illustrates the scenario when the Wi-Fi beacon transmission falls within the boundaries of the LAA transmissions period, as shown in Fig 8 (Case 3). For instance, the beacon transmitted can overlap either with the beginning of LAA transmission *i.e,* LAA waits for CCA duration and starts data transmission, which hinders the ongoing Wi-Fi beacon transmission. Also, a beacon transmission can prolong after LAA transmission *i.e.,* Wi-Fi starts a beacon transmission during an ongoing LAA transmission and continues until some part of the LAA CCA duration. In both cases, we receive the beacon successfully, even when it has minimal overlap with LAA transmission.

Such overlapping of broadcast packets with LAA transmission does not let the hidden Wi-Fi node/STA be aware of a Wi-Fi access point, increasing the scanning time, thereby accounting for longer association time.

5.1.2. Data Packet Transmission

This section captures the issues with data packet transmission which analyzed in the following four scenarios

- *LAA transmission collides with Wi-Fi Data/Wi-Fi ACK:* Like the beacon collision, LAA's transmission can collide with the Wi-Fi data transmission. The packets originating from the Wi-Fi Access point intended to be received by the hidden node suffer collision, as shown in Fig. 10 (Scenario 1). Which lengthens the time to get a packet delivered successfully to the hidden Wi-Fi node/STA. Since Wi-Fi AP cannot sense LAA transmission and the LAA transmitter's inability to detect RTS/CTS from Wi-Fi nodes/STAs, this scenario is challenging. The packets intended to be received by the hidden node always suffer a collision if there is an LAA transmission.

- *LAA defers transmission of hidden Wi-Fi nodes/STAs:* In the scenario shown in Fig. 10 (Scenario 2), Wi-Fi AP and LAA nodes/BSs cannot listen to each other. The Wi-Fi in the hidden region can also hear both LAA and Wi-Fi AP/other stations transmission in the channel. A packet originating at a hidden Wi-Fi station waits for DIFS + back-off (BO) time before it can start its transmission. It is improbable to find DIFs time the channel to be Idle, *i.e.,* without any other Regular Wi-Fi node's/STAs transmission and LAA transmission. If the DIFS time in the Wi-Fi. ambit and CCA time in LAA ambit not aligned, then the hidden nodes have to wait until these times overlap for DIFS duration, after which it can count for the back-off duration.

- *Wi-Fi Data and ACK fall on the LAA packet transmission boundaries:* Wi-Fi Data or ACK originated from Wi-Fi AP/Regular Wi-Fi nodes/STAs targeted to be received by hidden Wi-Fi nodes/STAs suffers high interference if the packet falls on the LAA transmission boundaries as shown in Fig. 11 (Scenario 3). Unlike the broadcast packets, these collisions stall the Wi-Fi AP/regular nodes until the packet is successfully delivered to the hidden nodes, or the maximum retransmission limit is met.
- *Successful Data/ACK reception to Hidden Wi-Fi within LAA CCA:* The hidden Wi-Fi node/STA can successfully decode a Data/ACK only when the packet is delivered during LAA CCA time or when there is no transmission in the LAA ambit, as shown in Fig. 11 (Scenario 4).

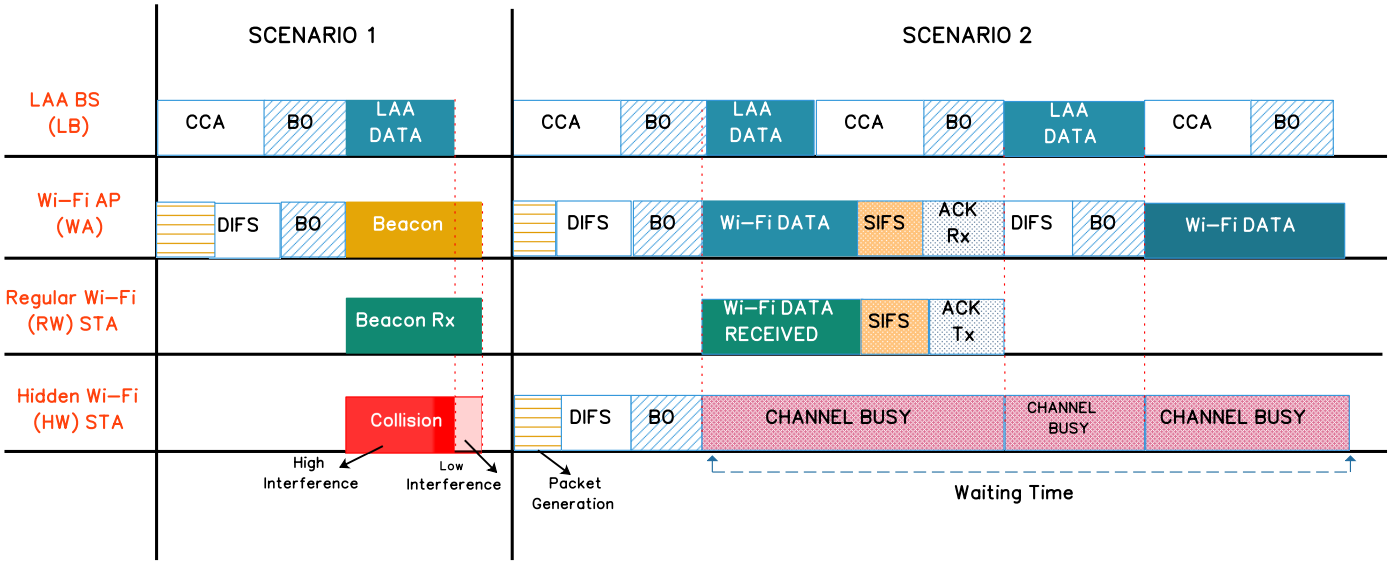

Figure 10: *Scenario 1 and Scenario 2:* LAA Wi-Fi Coexistence Data & ACK Transmission

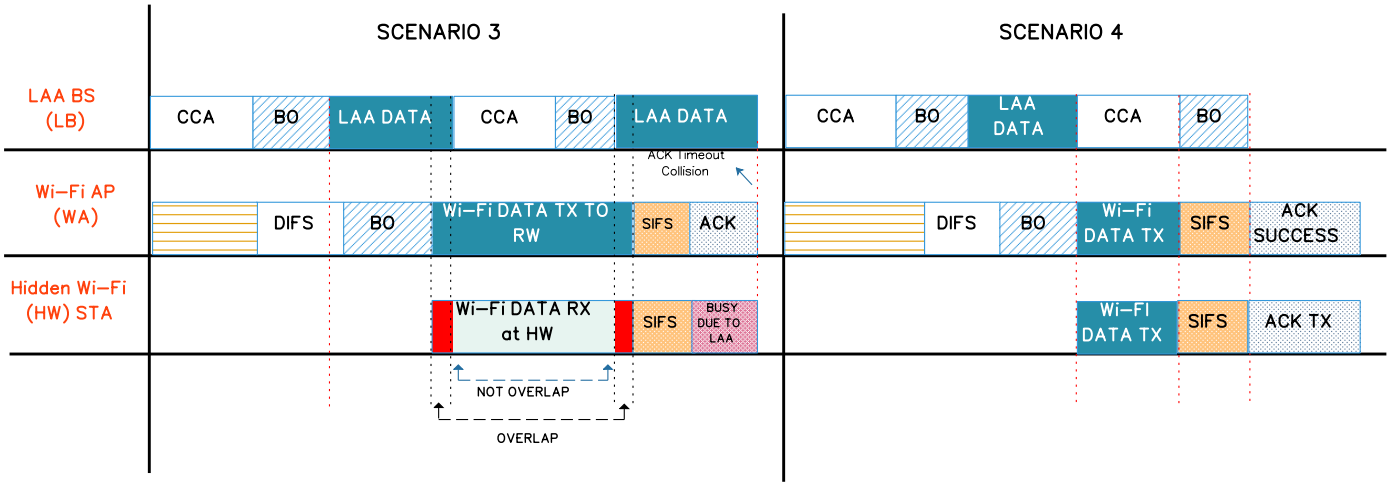

Figure 11: *Scenario 3 and Scenario 4:* LAA Wi-Fi Coexistence Data & ACK Transmission

5.2. Analysis of hidden Wi-Fi station in LAA Ambit

This section describes the analytical model for a scenario that includes a set of Wi-Fi stations hidden from LAA nodes. Fig. 9 captures the hidden Wi-Fi scenario. The scenario includes a set of LAA UEs associated with LAA BS

and Wi-Fi stations associated with a Wi-Fi AP. Some of those Wi-Fi stations fall within the communication range of LAA *i.e.,* some Wi-Fi nodes/STAs can listen to LAA transmission. Nevertheless, the LAA nodes are unaware of Wi-Fi nodes/STAs in their communication region due to the higher Energy Detection (ED) threshold. This work includes the following assumptions

- There are no hidden Wi-Fi nodes/STAs in the Wi-Fi ambit. Each Wi-Fi node/STA can hear from the rest of the Wi-Fi nodes/STAs
- LAA nodes are visible within LAA ambit *i.e.,* Every LAA node can hear every other LAA node in the channel
- Some Wi-Fi nodes/STAs fall in the LAA node's transmission region, *i.e.,* some Wi-Fi stations can listen to LAA transmission. But LAA nodes cannot hear these Wi-Fi transmissions These nodes are hidden nodes in this work

This analytical model targets to capture the throughput performance of the Wi-Fi network due to the hidden Wi-Fi nodes/STAs.

5.3. Modeling assumptions

There are N nodes *i.e.,* Wi-Fi and LAA in the system ($N = n_W + n_L$) where n_W is the number of Wi-Fi nodes/STAs and n_L is the number of LAA nodes. The notation and abbreviation used in the modeling are described in Table. 4.

$$\tau_W = \frac{2}{W_0\left[\frac{(1-(2P_W)^{m+1})(1-P_W)+2^m(P_W^{m+1}-P_W^{m+2})(1-2P_W)}{(1-2P_W)(1-P_W^{m+2})}\right]+1} \tag{1}$$

τ_W corresponds to the probability that a Wi-Fi node/STA will transmit in a time slot (obtained from [6]). P_W corresponds to the possibility that a transmitted packet from the Wi-Fi node/STA will collide. m refers to maximum back-off stages. W_o and $W_0^{'}$ values are set to 16.

The transmission probability of the LAA node (τ_L) obtained form [6]

$$\tau_L = \frac{2}{W_0'\left[\frac{(1-P_L)(1-(2P_L)^{m'+1})}{(1-2P_L)(1-P_L^{m'+e_l+1})}+2^{m'}\frac{P_L^{m'+1}-P_L^{m'+e_L+1}}{1-P_L^{m'+e_L+1}}\right]+1} \tag{2}$$

Duration of successful data transmission (T_s^D) in Wi-Fi ambit can be expressed as

$$T_s^D = H + E[PD] + SIFS + \delta + ACK + DIFS + \delta \tag{3}$$

E[PD] is the expected duration of packets in time, and H refers to Header length in time. Time incurred in the successful delivery of Beacon transmission (T_s^B) can be expressed as

$$T_s^B = H + E[PD] + DIFS + \delta \tag{4}$$

The duration of a collision (T_c) event can be expressed as

$$T_c = H + E[PD] + DIFS + \delta \tag{5}$$

Table 4: Symbols used in Coexistence Modeling

Parameter	**Notation**
Number of Nodes in the system	N
Contention window size of Wi-Fi in the i^{th} back-off	W
Number of Wi-Fi nodes/STAs	n_W
Number of LAA nodes	n_L
Transmission probability of Wi-Fi ambit	τ_W
Packet collision probability in Wi-Fi ambit	P_W
Maximum back-off stages	m
Probability of any transmission in the channel	P_{tr}
Probability of successful tx in Wi-Fi ambit	P_S^W
Transmission probability of LAA	τ_L
Expected duration of packet	$E[PD]$
Packet collision probability for hidden Wi-Fi node/STA	P^H
Packet collision probability for a regular Wi-Fi node/STA	P^R
Probability of any transmission in Wi-Fi ambit	P_{tr}^W
Duration of successful user data transmission	T_s^D
Time duration of successful beacon transmission	T_s^B
Probability of user data transmission	P_D
Probability of beacon transmission	P_B
Number of hidden nodes in Wi-Fi Ambit	n_H
Number of regular nodes in Wi-Fi ambit	n_R
Time duration of a time slot	T
i^{th} back-off Stage	$b_{i,0}$
Expected number of back off stages	$E[Nt_W]$
Expected duration of Frozen back off	$E[N_F r]$
Expected duration of Idle time	$E[Idle]$
Length of Header	H

5.4. Analyzing the performance in Wi-Fi Ambit

This section confines the investigation of Wi-Fi performance. The number of nodes in Wi-Fi ambit is given by (n_W) $n_W = n_H + n_R$ Here, n_H refers to several hidden Wi-Fi nodes/STAs (nodes that are affected by LAA transmission), and n_R corresponds to the regular Wi-Fi nodes/STAs which are not affected by the LAA transmission. Probability of a successful transmission within Wi-Fi ambit (P_s^W) expressed as

$$P_s^W = \left[\frac{n_H \tau_W (1-\tau_W)^{n_W-1} (1-\tau_L)^{(n_L I)} + n_R \tau_W (1-\tau_W)^{n_W-1}}{P_{tr}^W} \right] \tag{6}$$

P_s^W includes the hidden and regular Wi-Fi transmissions, I corresponds to the number of slots the LAA nodes should be idle in order to make the hidden Wi-Fi transmission to be successful. Typically I corresponds to twice the length of a Wi-Fi transmission ($I = 2T_s/T$). The probability that a node in Wi-Fi ambit transmits (P_{tr}^W) can be given by

$$P_{tr}^W = 1 - (1-\tau_W)^{n_W} \tag{7}$$

A slot duration (T) in Wi-Fi ambit can be expressed as the sum of a collision event, successful event, and idle time with their corresponding probabilities

$$T = (1 - P_{tr}^W)\sigma + P_{tr}^W [P_s^W [T_s^D P_D + T_s^B P_B] + (1 - P_s^W) T_c] \tag{8}$$

P_D and P_B correspond to the probabilities that a transmission is a data and beacon respectively.

To obtain the value of I in terms of probabilities and τ_W, substitute, $T_s^D = \alpha\sigma$; $T_s^B = \beta\sigma$; $T_c^D = \gamma\sigma$ in the above equation

$$T = \sigma[(1 - P_{tr}^W) + P_{tr}^W [P_s^W (P_D \alpha + P_B \beta) + (1 - P_s^W)\gamma]] \tag{9}$$

α, β, and γ are constants. On further simplifying the above equation,

$$1 - \frac{T}{\sigma} = P_{tr}^W - P_s^W P_{tr}^W (P_D \alpha + P_B \beta - \gamma) - P_{tr}^W \gamma \tag{10}$$

Substitute, $T = 2T_s/I$; $T_s = \alpha\sigma + \beta\sigma$

The collision probability of the packet intended to be received by the hidden node can be expressed as

$$P^H = 1 - [(1-\tau_W)^{n_W-1} (1-\tau_L)^{n_L I}] \tag{11}$$

The collision probability of a packet to a regular Wi-Fi node/STA can be represented as

$$P^R = 1 - (1-\tau_W)^{n_W-1} \tag{12}$$

In case of saturated analysis collision probability of a transmitted packet in Wi-Fi ambit can be obtained as a weighted sum of packet collision at the hidden node and regular node collision

$$P_W = \frac{n_H}{n_H + n_R} P^H + \frac{n_R}{n_H + n_R} P^R \tag{13}$$

substituting P^H and P^R in eqn 6

$$P_s^W P_{tr}^W = n_H \tau_W (1 - P^H) + n_R \tau_W (1 - P^R) \tag{14}$$

substituting eqn (14) in eqn (10);

Number of slots the LAA node should be idle to make the hidden Wi-Fi node/STA transmission successful given in terms of τ and p in eqn (15)

$$I = \frac{2(\alpha+\beta)}{[[n_H\tau_W(1-P^H)+n_R\tau_W(1-P^R)](P_D\alpha+P_B\beta-\gamma)+[1-(1-\tau^W)^{n_W}](\gamma-1)]} \tag{15}$$

Saturation Throughput (S) of Wi-Fi ambit is given as

$$S = \frac{E[P]P_s^W P_{tr}^W}{T} \tag{16}$$

5.4.1. Convergence of τ_W and p

It is important to understand the convergence of τ_W and P_W. It is clear from [6] that τ_L and P_L converge. The value of τ_W can be obtained in terms of P_W by solving the eqn 13.

$$\tau_W^*(P_W) = 1 - \left[\frac{f_h + f_r - P_W}{f_h + f_r L}\right]^{\frac{1}{n_W-1}} \tag{17}$$

In eqn (17), f_r and f_h corresponds to the fraction of regular and hidden nodes. 0< f_h , f_r < 1, also f_h + f_r =1; n_W is the number of Wi-Fi nodes, n_W >= 2. Here $f_h = \frac{nH}{nH+nR}$ corresponds to fraction of hidden nodes; $f_r = \frac{nR}{nH+nR}$ corresponds to fraction of regular nodes in Wi-Fi ambit. $L = (1-\tau_L)^{n_L I}$. Solving the eqn 17 with $P_W = 0$, yields,

$$\tau_W^*(0) = 1 - \left[\frac{f_h + f_r}{f_h + f_r L}\right]^{\frac{1}{n_W-1}} \tag{18}$$

solving τ_W^* with $P_W = 1$

$$\tau_W^*(1) = 1 - \left[\frac{f_h + f_r - 1}{f_h + f_r L}\right]^{\frac{1}{n_W-1}} \tag{19}$$

τ_W and P_W are dependent on each other. τ_W in eqn (1) decreases monotonically when P_W is changing from (0 to 1). $\tau_W(P_W)$ from eqn (17) is a monotonically increasing function in the interval 0 to 1. Hence we can get a unique solution from it. τ_W is monotonically decreasing function. By changing P_w from 0 to 1, keeping all other variables unchanged, we show in eqn (18) and (19) that τ_w (0) < τ_w (1), hence we claim eqn 17 to be increasing monotonically.

5.4.2. Delay Incurred in a Successful Packet Delivery in Wi-Fi Ambit

This section investigates the delay incurred by a packet from the head of the device queue until successful delivery at the destination. Delay committed for a successful packet delivery can be expressed as a sum of the following (1) Idle time spent by that node during back off decrements, (2) Waiting time incurred during other nodes transmissions, and (3) Time incurred in a successful packet transmission by that node, the delay s obtained by extending the delay analysis in [38]

$$E[D_W] = E[Nt_W]\sigma + E[N_{Fr}][P_s^W[T_s^D P_D + T_s^B P_B] + (1-P_s^W)T_c] + E[T_s] \tag{20}$$

$E[Nt_W]$ is the expected number of back-off stages a node has gone through before a successful transmission. $E[N_{Fr}]$ corresponds to the back-off frozen time.

$$E[Nt_W] = \sum_{i=0}^{m}\left(\frac{b_{i,0}}{\tau_W}\frac{W_{i-1}}{2}\right) \tag{21}$$

Frozen time ($E[N_{Fr}]$) can be expressed as

$$E[N_{Fr}] = \frac{E[Nt_W] - E[Idle]}{E[Idle]} \tag{22}$$

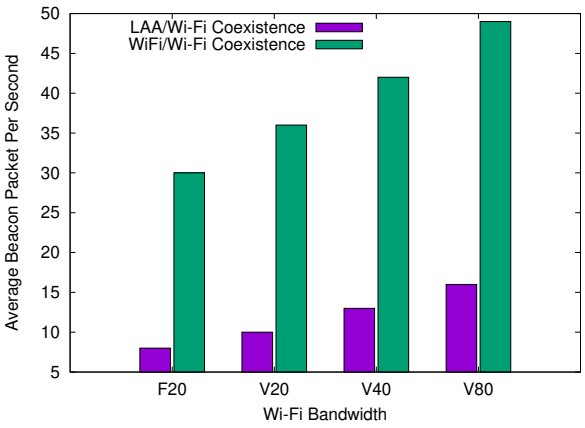

Figure 12: Successful Wi-Fi Beacon Transmission

$E[Idle]$ corresponds to the expected idle time of a node. It can be given as follows.

$$E[Idle] = \frac{1 - P_{tr}^{W}}{P_{tr}^{W}} \tag{23}$$

6. Experiment Results and Analysis

In this section, we present the results of our experiments and our analysis for the association for Wi-Fi and data transmission for LAA and Wi-Fi, first on the Wi-Fi side association, then on the LAA and Wi-Fi side data transmission.

6.1. Real-time Issues in Wi-Fi Association Process

In this section, we discuss the impact of Wi-Fi association packets such as beacon transmission, probe packets, authentication, association, and disassociation in LAA coexistence.

Beacon Transmission: Fig. 12 shows the average beacon transmission in seconds for the different Wi-Fi wider bandwidths F20, V20, 40, and 80 MHz. In the F20 scenario, all the 5 Wi-Fi APs and 5 Wi-Fi clients operate on the same channel 36 (where T- Mobile LAA operates on channels 36, 40, and 44). We observe in Wi-Fi to Wi-Fi coexistence scenario, all the Wi-Fi beacon packets from AP are transmitted more than the LAA to Wi-Fi coexistence. Similarly, in V20, all Wi-Fi APs are deployed in all T-Mobile LAA channels 36, 40, and 44, so the Wi-Fi loads are distributed on all LAA channels. Hence, this provides an opportunity for a more successful beacon transmission compared to the F20 scenario. As the Wi-Fi APs deployed on the wider bands like 40 and 80 MHz. We observe more number of successful Wi-Fi beacons compared to the narrow 20 MHz bands.

Probe Request and Probe Response: In this Section, we consider the F20 scenario for Wi-Fi/Wi-Fi and LAA/Wi-Fi scenario because we are interested in focusing on much detail on how the association process impacts the Wi-Fi LAA coexistence in a hidden situation. Fig. 13 shows the broadcast packet of the Wi-Fi client probe request (as represented in a red square), and corresponding probe response packets are shown in green color for the F20 deployment of Wi-Fi to Wi-Fi coexistence. Fig. 14 shows the probe request and probe response on F20 for LAA to Wi-Fi coexistence. We can see more number of probe responses to the corresponding probe request for LAA Wi-Fi coexistence. The probe response is a unicast packet; hence for unsuccessful transmission, the Wi-Fi AP tries several attempts to retransmit. This behavior is worse compared to Wi-Fi Wi-Fi coexistence.

Authentication and Association: Fig. 15 and 16shows the authentication and deauthentication packets for Wi-Fi/Wi-Fi to LAA/Wi-Fi coexistence. We observe more number of authentication and deauthentication packets when

LAA coexists with the Wi-Fi AP. This is because these packets are unicast and did not get an opportunity at Wi-Fi AP to transmit due to the maximum TXOP at LAA BS *i.e.,* 8 ms. Fig. 17 and 18 shows the association request and association response packet on Wi-Fi/Wi-Fi and LAA/Wi-Fi coexistence. In Wi-Fi/Wi-Fi coexistence, we can observe an equal number of association response packets for the corresponding association request. Hence, there is a lesser number of packet drop in association request due to the fairness of CSMA/CA used in Wi-Fi/Wi-Fi coexistence. On the contrary, we can observe less association response packets in LAA/Wi-Fi coexistence due to a hidden node scenario and the incompatibility of CSMA/CA and LBT mechanisms, which then lead to client disconnection on Wi-Fi side. Next, Fig. 19 and 20 show the reassociation request and association response for the Wi-Fi/Wi-Fi and LAA/Wi-Fi coexistence. We can observe more reassociation packets in LAA/Wi-Fi coexistence than the Wi-Fi/Wi-Fi coexistence, which further indicates a higher number of disconnection due to the adverse effect of hidden node problem in LAA/Wi-Fi coexistence.

Disassociation and Connection Failure: Fig. 21 and 22 shows the number of disassociation packets on Wi-Fi/Wi-Fi and LAA/Wi-Fi coexistence. We observe higher number of Wi-Fi client disassociation to the AP in LAA/Wi-Fi coexistence compared to the Wi-Fi/Wi-Fi coexistence. It is clear that when LAA coexists with Wi-Fi AP in the hidden node scenario, then the Wi-Fi client faces a hard time associating with its AP. Fig. 23 shows the total number of connection failures observed over the experiment duration of 2 minutes for each scenario. We observe an overall reduction in the number of connection failures as Wi-Fi APs operates on the wider band.

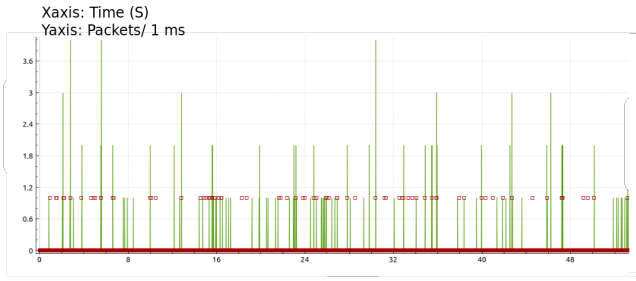

Figure 13: *Probe Request and Probe Response on Fixed 20 MHz:* Wi-Fi to Wi-Fi Coexistence

Figure 14: *Probe Request and Probe Response on Fixed 20 MHz:* LAA to Wi-Fi Coexistence

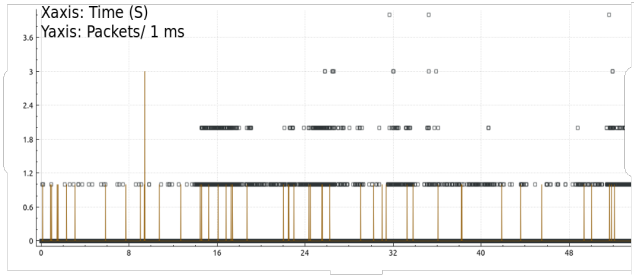

Figure 15: *Authentication and De-authentication on Fixed 20 MHz:* Wi-Fi to Wi-Fi Coexistence

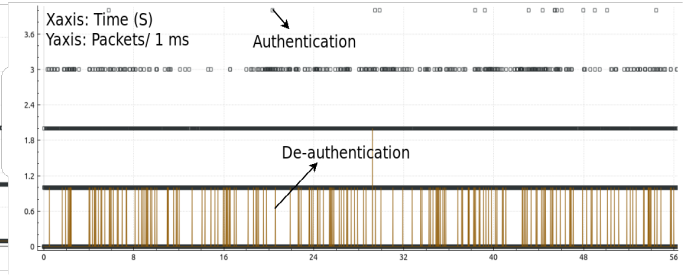

Figure 16: *Authentication and De-authentication on Fixed 20 MHz:* LAA to Wi-Fi Coexistence

6.2. LAA/Wi-Fi Coexistence at LAA side: Data Transmission

In this experiment, the LAA client initiates different kinds of traffic such as Data (D), Data + Video (D+V), Streaming (S), Data + Streaming (D+S), Video (V). We observe the System's performance at University (*i.e.,* IIT campus where T-Mobile operator deployed its LTE and LAA BS. The licensed spectrum of T-Mobile in this location is 15 MHz bandwidth (*i.e.,* maximum of 75 Physical Resource Blocks (PRBs) in LTE) and the LAA can support a maximum of 3 unlicensed carriers (each carrier is a maximum of 20 MHz bandwidth) in the 5 GHz channel of 36, 40 and 44. The maximum T-Mobile can have, including licensed and unlicensed spectrum, is 75 MHz (*i.e.*, 375 PRBs).

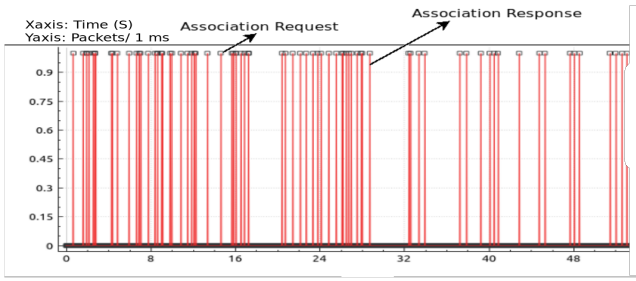

Figure 17: *Association Request and Response on Fixed 20 MHz:* Wi-Fi to Wi-Fi Coexistence

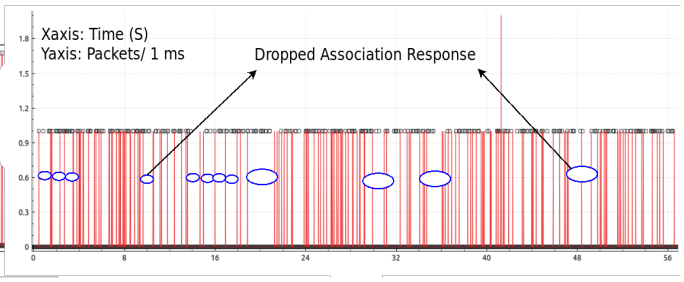

Figure 18: *Association Request and Response on Fixed 20 MHz:* LAA to Wi-Fi Coexistence

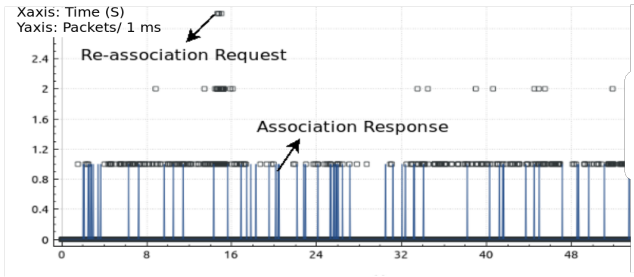

Figure 19: *Re-association request and association response on Fixed 20 MHz:* Wi-Fi to Wi-Fi Coexistence

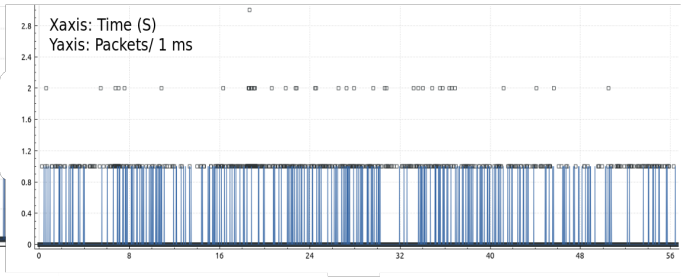

Figure 20: *Re-association request and association response on Fixed 20 MHz:* LAA to Wi-Fi Coexistence

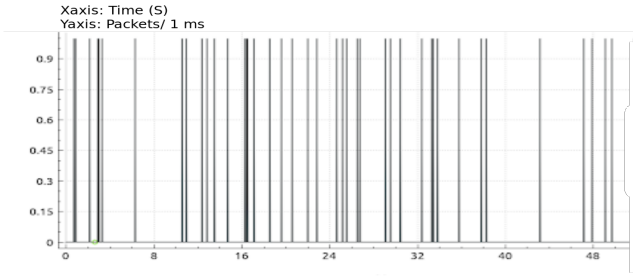

Figure 21: *Disassociation Process on Fixed 20 MHz:* Wi-Fi to Wi-Fi Coexistence

Figure 22: *Disassociation Process on Fixed 20 MHz:* LAA to Wi-Fi Coexistence

The spectrum allocation in unlicensed bands is enormous compared to the licensed spectrum. In this setup, we used a Google Pixel 3 phone that supports LAA on band 46 and the Network Signal Guru[3] tool which provides the details of PRBs, and throughput allocated per channel.

As of the time of experiments, we observed minimal LAA usage in downtown Chicago, possibly because only a few phones at the time are LAA-capable and tend to be more expensive. In many cases, ours was the only LAA phone in the cell, since all available resource blocks were allocated to our device during D traffic experiments (as reported by the Network Signal Guru app). It allows us to perform a controlled analysis as follows. First, we turn LAA ON (*i.e.,* the Google Pixel 3 and Samsung phone connected to the unlicensed component carrier of LAA) and requested different types of traffic transmission. In this case, we observe a fewer number of Wi-Fi APs on the same channel. Next, we find the Wi-Fi/Wi-Fi coexistence scenario without LAA (i.e., no LAA unlicensed component carrier turned ON) and requested the same type of traffic transmission using Wi-Fi.

[3]https://m.qtrun.com/en/product.html

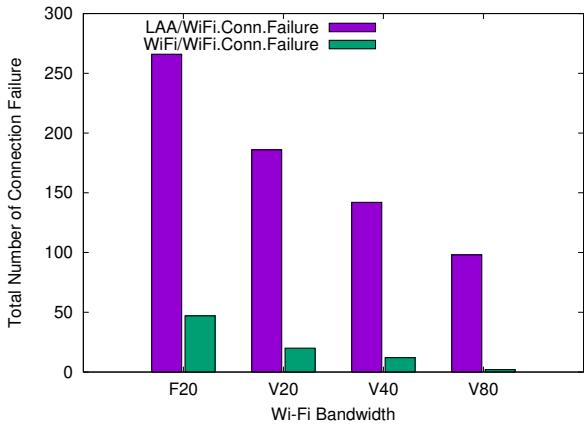

Figure 23: Unsuccessful Wi-Fi client Connections

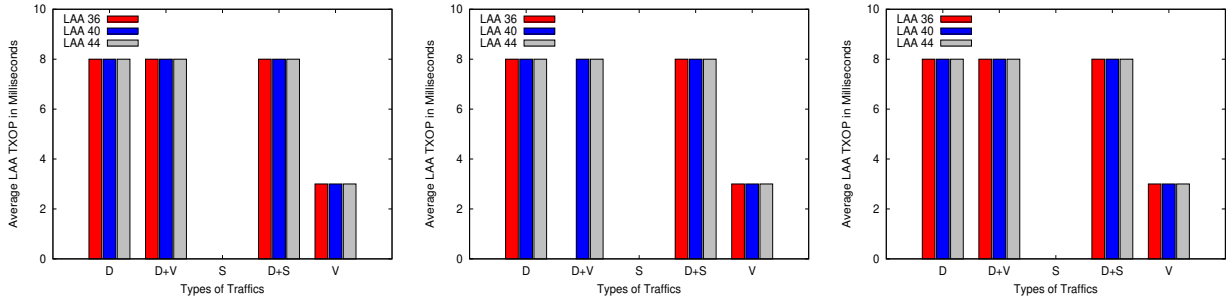

(a) LAA Base Scenario (b) LAA/Wi-Fi Coexistence (F20) (c) LAA/Wi-Fi Coexistence (V20)

Figure 24: TXOP: LAA/Wi-Fi Coexistence at LAA Side

6.2.1. Transmission Opportunity (TXOP)

We define the LAA base scenario where there is no Wi-Fi AP on channels 36, 40, and 44, as shown in Fig. 24 (a). When an LAA client connects to a nearby LAA BS for data access, we observe a TXOP of 8 ms. Likewise, whenever the data is associated with the video and streaming, operators use the maximum TXOP. For video traffic (*i.e.,* YouTube), we observe the maximum transmission opportunity of 3 ms. Meanwhile, we observe no unlicensed transmission in LAA for the streaming application, *i.e.,* LAA BS only uses licensed spectrum. In F20 and V20 scenario, we observe TXOP values similar to the LAA base case scenario. Fig. 24 (b) and 24 (c) show the TXOP of LAA/Wi-Fi coexistence at the LAA side; we observe the same number of TXOP for all traffics is similar to the LAA base case. Hence, we infer that LAA is not aware of Wi-Fi AP transmission in the hidden node scenario. We also observe no transmission in the F20 cases on the D+V scenario.

6.2.2. SINR

In the LAA base case, we observe SINR for the three different channels, as shown in Fig 25 (a). The reason for fluctuating SINR values is due to interference, distance, and path loss due to trees, snow, vehicles, and other objects. When we observe the F20 scenario, D+V traffic on channel 36 has a poor SINR value of -2.2 dB for LAA/Wi-Fi coexistence. As shown in Fig. 25 (b) on the F20 scenario, the SINR value is poor on channel 36 for all traffic because of interference from the deployed Netgear Wi-Fi APs. However, the channels 40 and 44 on F20 scenarios can observe better SINR because there are no Wi-Fi APs deployed on those channels. It is not the case for V20 scenarios (as shown in Fig. 25 (c)), The Wi-Fi APs deployed on all three channels 36, 40, and 44 such that the load is distributed on all three different channels, thus the poor SINR is observed in all three channels.

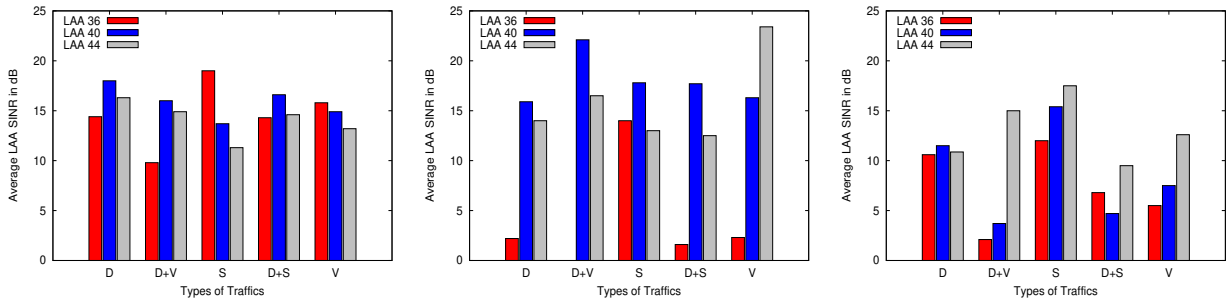

(a) LAA Base Scenario (b) LAA/Wi-Fi Coexistence (F20) (c) LAA/Wi-Fi Coexistence (V20)

Figure 25: SINR: LAA/Wi-Fi Coexistence at LAA Side

Table 5: LAA Base Scenario

Traffics	**LAAC36**	**LAAC40**	**LAAC44**
D	64 QAM	64 QAM	64 QAM
D + V	64 QAM	64 QAM	64 QAM
S	N/A	N/A	N/A
D + S	64 QAM	64 QAM	64 QAM
V	64 QAM	64 QAM	64 QAM

6.2.3. Modulation Coding Scheme (MCS)

Table 5 clearly shows that in the LAA Base case, all traffics is transmitted using a decent MCS (*i.e.,* 64 QAM) due to no interference. As expected at the F20 scenario, as shown in Table 6, we observe lower MCS on channel 36 (*i.e.,* QPSK) because of massive interference from the Wi-Fi APs to LAA client that leads to low SINR and directly relates to the lower MCS assignment. For V20 scenario, as shown in Table 7, the modulation coding scheme is distributed evenly to all the three different unlicensed channels. Note that T-Mobile LAA is capable of 256-QAM modulation when the LAA client SINR > 28 dB. As we are far away from the LAA BS, we did not observe the maximum MCS.

6.2.4. Resource Blocks (RBs)

Fig. 26 (a), 26 (b), and 26 (c) show the unlicensed RB allocation in the LAA base case, LAA/Wi-Fi coexistence on the F20 scenario, and LAA/Wi-Fi coexistence on the V20 scenario, respectively. For the D, D + V, and D + S traffic, the maximum number of RBs is allocated on channels 36, 40, and 44. However, the Video traffic shows lower RB allocation compared to Data traffic due to the fixed number of video frames to be transmitted (*i.e.,* a constant bit rate). On the contrary, the LAA client demands more resources on Data traffic; hence all RBs are used (in this case, we are the only LAA client connected to the LAA BS). Similar to the previous work, we observe all RBs are allocated in the licensed spectrum for Streaming traffic, so we cannot observe any unlicensed RB allocation at the LAA BS.

6.2.5. Throughput

Fig. 27 (a) shows the LAA base case, where LAA throughput is high compared to Fig. 27 (b) and 27 (c) of LAA/Wi-Fi coexistence F20 and V20 scenarios, respectively. Though the RB allocation is the same for all D, D + V, and D + S traffic, there is a difference in throughput. This is due to the SINR variation on each unlicensed channel based on Wi-Fi co-channel interference, path loss, etc. which leads to lower MCS operation at the LAA BS, which in turn leads to lower throughput. For the Video traffic, we observe an overall lower throughput compared to other traffics due to the lesser RB allocation as shown in Fig. 26 (a), 26 (b) and 26 (c).

Table 6: LAA/Wi-Fi Coexistence (F20)

Traffics	LAAC36	LAAC40	LAAC44
D	QPSK	64 QAM	64 QAM
D + V	N/A	64 QAM	64 QAM
S	N/A	N/A	N/A
D + S	QPSK	64 QAM	64 QAM
V	QPSK	64 QAM	64 QAM

Table 7: LAA/Wi-Fi Coexistence (V20)

Table	LAAC36	LAAC40	LAAC44
D	16 QAM	16 QAM	16 QAM
D + V	QPSK	QPSK	64 QAM
S	N/A	N/A	N/A
D + S	16 QAM	16 QAM	16 QAM
V	16 QAM	16 QAM	64 QAM

6.2.6. Average Performance of LAA for Data Traffic

In this section, we are interested in observing the performance of LAA on data traffic (*i.e.,* for all three channels) coexisting with Wi-Fi with varying bandwidth, *i.e.,* 20, 40, and 80 MHz. Because in a realistic scenario, we observe Wi-Fi APs are deployed with varying bandwidths to improve the data rates of connected Wi-Fi clients. Fig. 28 (a) shows the average TXOP of 8 ms duration irrespective of the Wi-Fi bandwidth (from narrow to the broader band). This, in turn, makes the Wi-Fi transmission difficult in the hidden scenario. Similarly, we observe an average RB allocation of 100, as shown in Fig. 28 (b), irrespective of Wi-Fi bandwidth. Table 8 shows the average modulation coding scheme at the LAA side with different Wi-Fi bandwidths. Fig. 28 (c) shows the average throughput for different Wi-Fi bandwidths, but there is a fluctuation in data rate due to different SINRs on all three channels.

Table 8: Average Modulation Coding Scheme at LAA

Wi-Fi Bandwidth	LAA Base	LAA/Wi-Fi
20	64 QAM	QPSK
V20	64 QAM	16 QAM
40	64 QAM	64 QAM
80	64 QAM	64 QAM

6.3. LTE/Wi-Fi Coexistence at Wi-Fi side: Data Transmission

In this experiment, the Wi-Fi client initiates different kinds of traffic, similar to the LAA clients such as Data (D), Data + Video (D+V), Streaming (S), Data + Streaming (D+S), Video (V) which is similar to the LAA clients. We deployed 5 Wi-Fi AP and 5 Wi-Fi clients. In this setup, we used a Wireshark tool that can capture the Wi-Fi packets in the monitor mode (*i.e.,* to observe all packets to the configured channel in the air-medium) on channels 36, 40, and 44. All these Wi-Fi APs are connected to the IIT campus internet via the backhaul, and we try to ensure no other external Wi-Fi AP is operating on those three unlicensed channels (i.e., 36, 40, and 44).

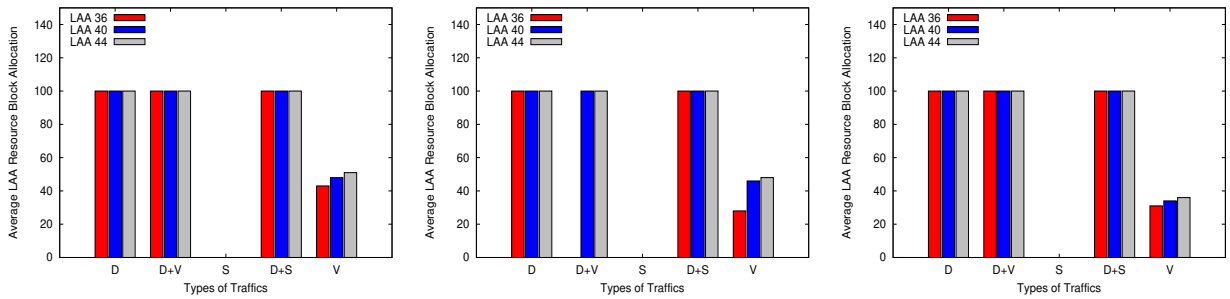

(a) LAA Base Scenario (b) LAA/Wi-Fi Coexistence (F20) (c) LAA/Wi-Fi Coexistence (V20)

Figure 26: RBs: LAA/Wi-Fi Coexistence at LAA Side

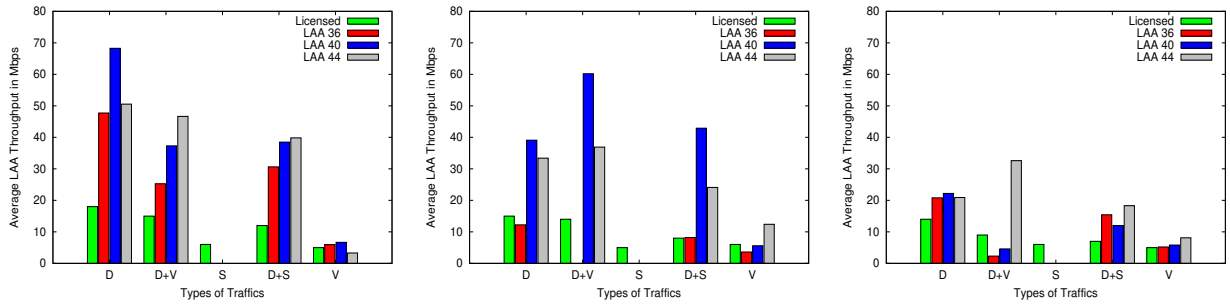

(a) LAA Base Scenario (b) LAA/Wi-Fi Coexistence (F20) (c) LAA/Wi-Fi Coexistence (V20)

Figure 27: Throughput: LAA/Wi-Fi Coexistence at LAA Side

6.3.1. Average Packet Transmission at Wi-Fi Side on Fixed 20 MHz Channel

Fig. 29 (a), 29 (b), and 29 (c) show the average packet transmission on F20 configuration for five different types of Wi-Fi traffics. On channel 36, we observe more Wi-Fi AP packets because all the 5 Wi-Fi APs and 5 Wi-Fi clients are deployed on it. On the other hand, we see less number of Wi-Fi packets in channels 40 and 44 (as shown in Fig. 29 (b) and Fig. 29 (c)), which consists of only control packets like probe request (transmitted by nearby random Wi-Fi clients). Similarly, Fig. 30 (a), 30 (b) and 30 (c) show the average data rate at the Wi-Fi side on a F20 channel. From Fig. 29 (a) and Fig. 30 (a), it's clear when LAA coexists with the Wi-Fi APs, the average number of packets transmitted per second and throughput is less compared to the Wi-Fi coexisting with the Wi-Fi AP. It shows the impact of LAA coexistence with the Wi-Fi AP.

6.3.2. Average Packet Transmission at Wi-Fi Side on Variable 20 MHz Channel

In this scenario, all Wi-Fi APs deployed on all three different channels, *i.e.,* 2 Wi-Fi AP on channel 36, 2 Wi-Fi AP on channel 40, and 1 Wi-Fi AP on channel 44. Fig. 31 (a), 31 (b), 31 (c) show the average packet transmission for variable 20 MHz on channels 36, 40, and 44. Similarly, Fig. 32 (a), 32 (b) and 32 (c) show the average data rate at the Wi-Fi side on a V20 scenario. We observe that the number of Wi-Fi packets and throughput is less when it coexists with the LAA. Hence, the hidden node plays a key role in both F20 and V20 scenarios.

LAA & Wi-Fi coexistence performance on Wi-Fi Wider Bandwidth: In this section, we discuss the LAA Wi-Fi coexistence on 80 MHz Wi-Fi bandwidth operation. Unfortunately, the Laptop in the Wi-Fi monitor mode captures only 20 MHz primary channels on 36, 40, and 44. Hence, this section's results discussion is mostly on Wi-Fi 80 MHz management packets and a small portion of data packets.

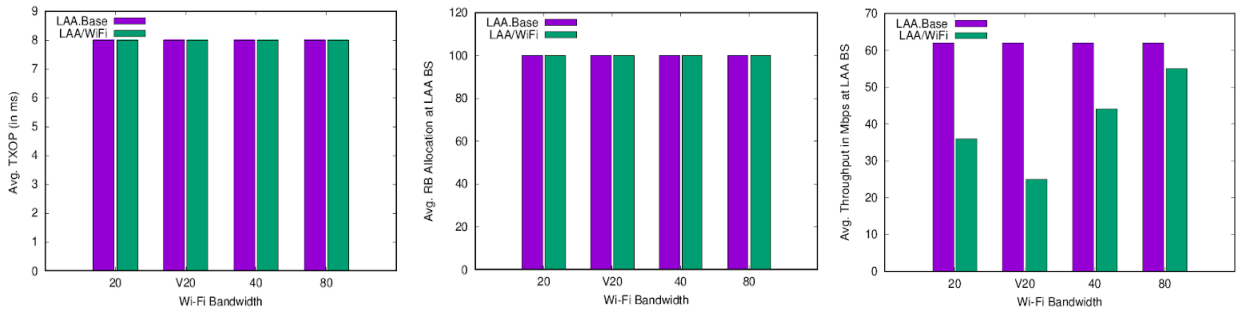

(a) Average TXOP at LAA (b) Average RB allocation at LAA (c) Average Throughput at LAA

Figure 28: Average Performance of LAA for Data Traffic

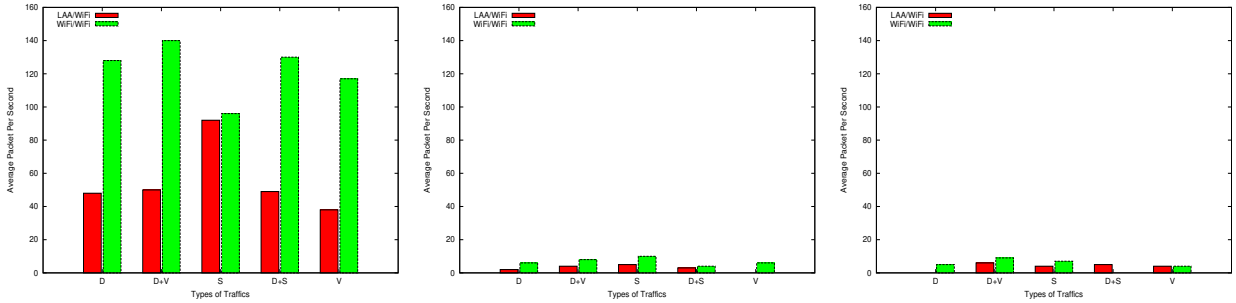

(a) All Wi-Fi at Channel 36 (b) All Wi-Fi at Channel 40 (c) All Wi-Fi at Channel 44

Figure 29: Average Packet Transmission at Wi-Fi Side on Fixed 20 MHz Channel

6.3.3. LAA Wi-Fi coexistence performance on Wider Bandwidth at 80 MHz Bandwidth

Fig. 33 (a) shows the average throughput on management and data packets observed at LAA when Wi-Fi AP operates on 80 MHz bandwidth, where 2 Wi-Fi AP operates on primary channel 36 and 2 Wi-Fi APs on channel 40, and one AP on channel 44. Unlike 20 and 40 MHz, the Wi-Fi AP has more opportunity to transmit the packet on the wider bands. This in turn reduces the impact of interference on the LAA. Hence, we observe better throughput at the LAA side compared to 20 MHz. Similarly, the Wi-Fi AP has more opportunity to transmit packets for all five different types of traffic (*i.e.,* D, D+V, S, D+S, V) as shown in Fig. 33 (b) compared to 20 MHz. This further improved the data rate at Wi-Fi AP as shown in Fig. 33 (c). The throughput observed at the Wi-Fi side is averaged over all Wi-Fi clients.

Performance of LAA Wi-Fi Coexistence at Wi-Fi Different Bandwidth: In this section, we discuss the average packet transmission, data rate, and MCS at different Wi-Fi bandwidths.

6.3.4. Average Packet Transmission on different Wi-Fi Bandwidth

Fig. 34 (a) shows the average packet transmission over the different Wi-Fi bandwidths: from narrow to broader bandwidths. As the Wi-Fi deployment moves from narrow to broader band, we observe more number of successful packet transmissions when LAA coexists with the Wi-Fi AP. The broader band allows the Wi-Fi APs to transmit more packets; hence, the average packet transmission per second is very high.

6.3.5. Average Data Rate and MCS on different Wi-Fi Bandwidth

Fig. 34 (b) shows the average data rate observed on Wi-Fi at different bandwidths. In Wi-Fi/Wi-Fi coexistence, We clearly observe higher throughput as the bandwidth increases. In LAA/Wi-Fi coexistence, we can see the impact of LAA on Wi-Fi data rates in different bandwidths. Fig. 34 (c) shows the modulation coding scheme (MCS) on

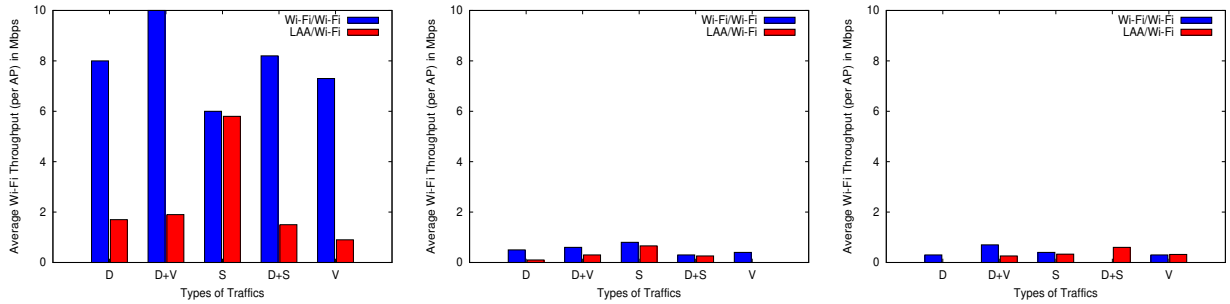

(a) All Wi-Fi at Channel 36 (b) All Wi-Fi at Channel 40 (c) All Wi-Fi at Channel 44

Figure 30: Average Throughput per AP at Wi-Fi Side on Fixed 20 MHz Channel

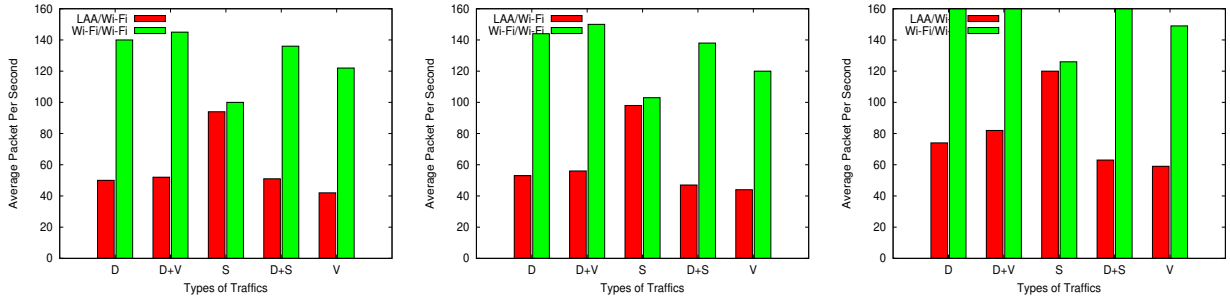

(a) Wi-Fi at Channel 36 (b) Wi-Fi at Channel 40 (c) Wi-Fi at Channel 44

Figure 31: Avg. Packet Transmission at Wi-Fi side on Variable 20 MHz Channel

Wi-Fi/Wi-Fi coexistence with decent coding schemes such as 16 QAM and 64 QAM. The MCS schemes used in LAA/Wi-Fi are lower (*e.g.,*BPSK and QPSK) compared to Wi-Fi/Wi-Fi.

7. Validation of Analytical model

This Section targets to validate the analytical model with simulation outcomes. The performance of all Wi-Fi nodes/STAs is captured with some of the nodes being hidden to LAA ambit. The simulation includes three categories of users, (1) Hidden Wi-Fi users, (2) Regular Wi-Fi users, and (3) LAA users. The following conditions are obeyed in the simulation,

- Hidden Wi-Fi users can listen to LAA users and Regular Wi-Fi users transmission.
- Regular Wi-Fi users can listen only to hidden Wi-Fi users transmission.
- LAA users can't listen to regular or hidden Wi-Fi users.
- A user of a category can listen to the transmission of another user belonging to the same category *i.e.* A hidden Wi-Fi user can listen to another hidden Wi-Fi user.

Normalized throughput is computed in all the experiments. Since this is a saturated throughput analysis, the user queue will be non-empty at all times. The simulation parameters are captured in Table 9.

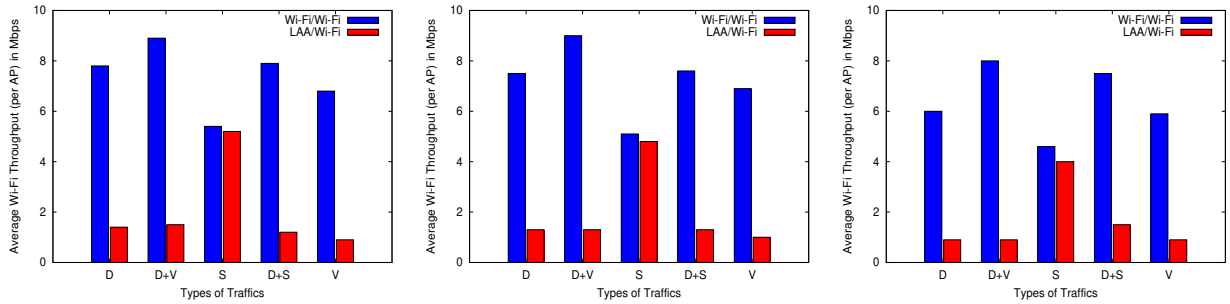

(a) Wi-Fi at Channel 36 (b) Wi-Fi at Channel 40 (c) Wi-Fi at Channel 44

Figure 32: Avg. Throughput per AP at Wi-Fi side on Variable 20 MHz Channel

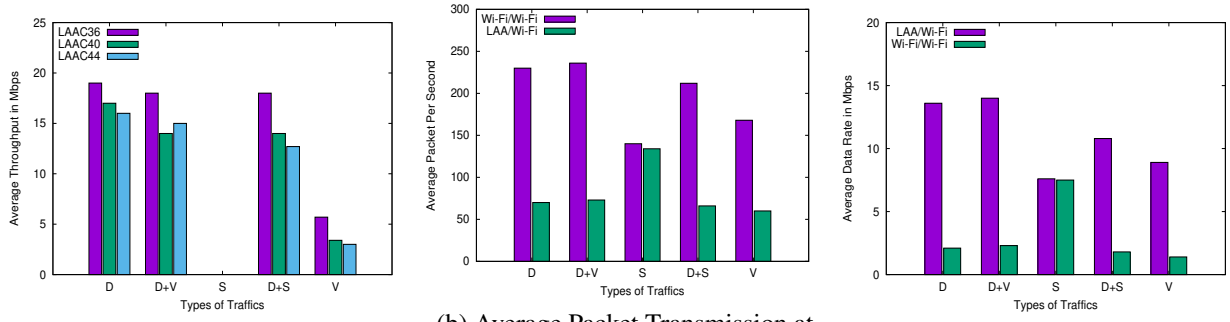

(a) Average Throughput at LAA (b) Average Packet Transmission at Wi-Fi (c) Average Throughput at Wi-Fi

Figure 33: Performance of LAA Wi-Fi Coexistence at Wi-Fi 80 MHz Bandwidth

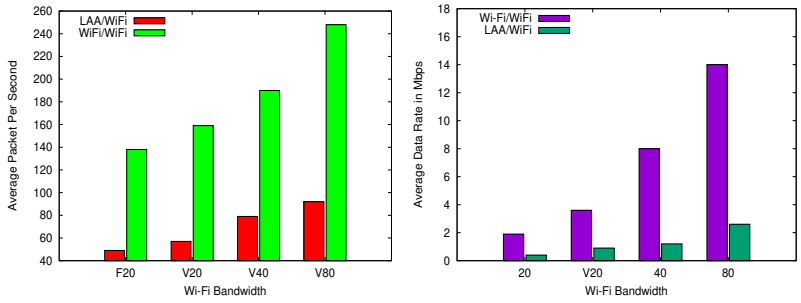

(a) Average Packet Transmission (b) Average Data Rate (Mbps)

Bandwidth	Wi-FI/Wi-Fi	LAA/Wi-Fi
20	16 QAM 1/2	BPSK 1/2
V20	16 QAM 3/4	BPSK 1/2
40	64 QAM 3/4	QPSK 3/4
80	64 QAM 3/4	16 QAM 3/4

(c) **Modulation Coding Scheme (MCS)**

Figure 34: Performance of LAA Wi-Fi Coexistence at Wi-Fi Different Bandwidth.

7.0.1. Throughput Analysis

Throughput was observed in the Wi-Fi ambit, with an increasing number of users in the network. The throughput is captured in the case of simulation and analysis. The simulation was conducted by varying the number of users from 16 to 40. Among the total number of users in the network, one-half of the users belong to the LAA ambit, and the other half belong to the Wi-Fi ambit. For instance, when 16 users are there in the network, there will be eight users in the Wi-Fi ambit, and eight users in the LAA ambit. Among eight users in the Wi-Fi ambit, four users will be hidden Wi-Fi, and the other four users will be regular Wi-Fi. Since we are interested in the performance of Wi-Fi due to the impact of LAA transmission, all our experiments capture only the performance of the Wi-Fi ambit.

In this setup, we vary the total number of Wi-Fi nodes in the network, the x-axis captures the number of Wi-Fi

Table 9: Simulation Parameters

Parameter	Value
SIFS	10 μsec
Slot time	9 μsec
DIFS	28 μsec
Channel Bit Rate	1 bits/μsec
propagation Delay	1 μsec
CW Min	16
CW Max	1024
Packet Payload Size	1024*8 bits
MAC Header	24*8 bits
PHY Header	16*8 bits

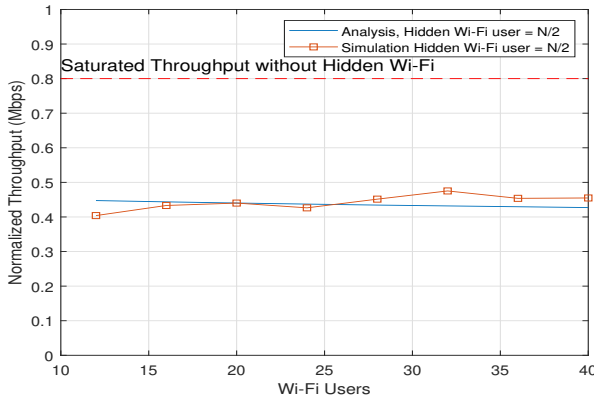

Figure 35: Throughput in Wi-Fi ambit.

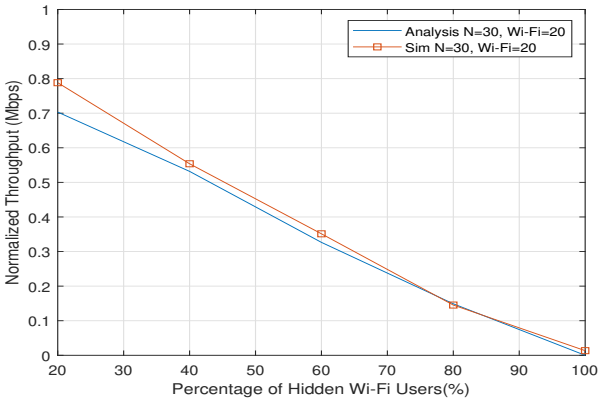

Figure 36: Throughput of Wi-Fi ambit with varying hidden Wi-Fi STAs.

nodes in the network. (*i.e,* 12, 16, 20, 24, 28, 32, 36, 40). Out of which half the users are considered to be hidden users, and the other half of the Wi-Fi users are regular (non-hidden) users. So, we have (*i.e.,* 6 hidden and 6 regular users for 12 Wi-Fi user data points). Fig. 35 captures the throughput of the Wi-Fi ambit with an increasing number of users in the network as the number of users increases the throughput of the network decreases. It includes the collision between Wi-Fi nodes/STAs and collisions due to LAA transmission. The experiment captures the actual performance degradation due to LAA. The experiment includes fixed users in the Wi-Fi ambit and the LAA ambit. Only the number of hidden Wi-Fi users and regular users within the Wi-Fi ambit is varied. For instance, the experiment sets the total number of Wi-Fi users in the network to be 20, out of which two users are hidden Wi-Fi, and the rest 18 are regular Wi-Fi. The experiment is repeated by increasing the number of hidden users from 2 to 20 in steps, while the regular users naturally decrease from 18 to zero. The aggregate throughput of the Wi-Fi users is almost half the total throughput of a non-hidden node scenario with saturated traffic (mentioned in the red line).

Fig. 36 capture the degradation in Wi-Fi throughput when the ratio of hidden Wi-Fi users is changed. In the experiment, we vary the ratio between hidden to total Wi-Fi users, from 20% to 100%. The aggregated throughput of the Wi-Fi nodes degraded linearly as the number of hidden Wi-Fi users increased in the system. As the hidden Wi-Fi users could listen to both LAA and regular Wi-Fi nodes/STAs simultaneously, they tend to wait longer before they get a transmission opportunity. Since the scenario considered here is a saturated case, the transmission opportunity is grabbed by LAA and regular Wi-Fi users aggressively, which leaves feeble or no opportunity for hidden users. There is no fair sharing of the channel within Wi-Fi under such a constrained scenario. Also, this long waiting time in case of hidden Wi-Fi prevents a new node from associating with a base station. Such association failures have a negative impact on battery usage [4, 9] as well. The association experiments conclude the same performance exhibited in real-time; the results are discussed in the above sections.

8. Conclusion

From these deployment maps, we can conclude that the LAA technology is successful and that the operators gain more benefits than the licensed spectrum. Nevertheless, the hidden node problem impacts Wi-Fi more compared to LAA. Furthermore, we can assume that this problem is more severe in a dense deployment like Chicago downtown, where the tall buildings could worsen the problem. We hope that the lessons learned from LAA coexistence will help the researchers to design a better coexistence framework for the eLAA deployment. Further, the analytical model can serve the purpose of understanding the extent of impact at the hidden Wi-Fi nodes/STAs.

Acknowledgement

We sincerely thank the Illinois Institute of Technology (IIT) campus authorities and departments for proving access in the campus property to conduct the realistic experiment.

References

[1] "LTE-U Forum, "LTE-U CSAT Procedure TS V1.0"." 2015.

[2] 3GPP Release 13 Specification, "http://www.3gpp.org/release-13/".

[3] N. Jindal, D. Breslin and A. Norman, "LTE-U and Wi-Fi: A Coexistence Study, White Paper," in *https://ecfsapi.fcc.gov/file/60001078145.pdf*.

[4] V. Sathya, M. Mehrnoush, M. Ghosh and S. Roy, "Analysis of CSAT Performance in Wi-Fi and LTE-U Coexistence," *Proc. IEEE Int. Conf. Commn.*, Kansas City, May 2018.

[5] M. Mehrnoush, S. Roy, V. Sathya and M. Ghosh, "On the Fairness of Wi-Fi and LAA Coexistence," in *IEEE Transactions on Cognitive Communications and Networking*, 2018.

[6] M. Merhnoush, V. Sathya, S. Roy, and M. Ghosh, "Analytical Modeling of Wi-Fi and LAA Coexistence: Throughput and Impact of Energy Detection Threshold", in *IEEE Transactions on Networking*, 2018.

[7] L. Li, J. P. Seymour, L. J. Cimini, and C. Shen, "Coexistence of Wi-Fi and LAA networks with adaptive energy detection," *IEEE Transactions on Vehicular Technology*, vol. 66, no. 11, pp. 10 384–10 393, Nov. 2017.

[8] H. Hu, C. Tan, M. Zheng, and F. Xie, "Contention window adaptation of listen-before-talk scheme for LTE and Wi-Fi coexistence in unlicensed spectrum," in *7th IEEE ICEIEC*, July 2017, pp. 61–65.

[9] Hu. Xueheng, Song. Lixing, Van. Bruggen, and Dirk. Striegel, "Is there wifi yet? how aggressive wifi probe requests deteriorate energy and throughput,", July 2015.

[10] Y. Gao, B. Chen, X. Chu, and J. Zhang, "Resource allocation in LAA and Wi-Fi coexistence: A joint contention window optimization scheme," in IEEE *GLOBECOM*, Dec. 2017, pp. 1–6.

[11] M.I. Rochman, V. Sathya, M. Ghosh, S. Roy, "LAA Cell Map," https://people.cs.uchicago.edu/muhiqbalcr/laa/, accessed March 2020

[12] V. Sathya, M. I. Rochman, and M. Ghosh, "Measurement-based coexistence studies of laa & wi-fi deployments in chicago," *IEEE Wireless Communication Magazine*, 2020.

[13] 3GPP, "Technical Specification Group Radio Access Network; Study on Licensed-Assisted Access to Unlicensed Spectrum;(Release 13)," *3GPP TR 36.889, V13.0.0*, June 2015.

[14] 3GPP, "LTE; evolved universal terrestrial radio access (E-UTRA); physical layer procedures (Release 10)," June 2011.

[15] S. Lagen, L. Giupponi, S. Goyal, N. Patriciello, B. Bojovic, A. Demir and M. Beluri, "New Radio Beam-based Access to Unlicensed Spectrum: Design Challenges and Solutions," in *IEEE Communications Surveys & Tutorials*, 2019.

[16] A. V. Kini, L. Canonne-Velasquez, M. Hosseinian, M. Rudolf, and J. Stern-Berkowitz, "Wi-fi-Laa coexistence: Design and evaluation of listen before the talk for Laa," in *2016 Annual Conference on Information Science and Systems (CISS)*, pp. 157–162, March 2016.

[17] T. Tao, F. Han, and Y. Liu, "Enhanced Lbt algorithm for LTE-Laa in unlicensed band," in *2015 IEEE PIMRC*, pp. 1907–1911, 2015.

[18] M.I. Rochman, V. Sathya, and M. Ghosh, "Impact of changing energy detection thresholds on fair coexistence of Wi-Fi and LTE in the unlicensed spectrum," in *IEEE WTS*, pp. 1–9, 2017.

[19] S. Hong, L. Giupponi, H. Lee, H. Kim, and H. Yang, "Lightweight Wi-Fi Frame Detection for Licensed Assisted Access LTE," in *IEEE Access*, pp. 77618–77628, 2019.

[20] Q. Chen, G. Yu, H. Lee, and Z. Ding, "Enhanced LAA for unlicensed LTE deployment based on TXOP contention," in *IEEE Transactions on Communications*, pp. 417–429, 2018.

[21] Y. Gao, G. Yu, and S. Roy, "Achieving Proportional Fairness for LAA and Wi-Fi Coexistence in Unlicensed Spectrum," in *IEEE Transactions on Wireless Communications*, 2020.

[22] H. Lee, and H. Yang, "Downlink Interference Control of LAA for Coexistence With Asymmetric Hidden Wi-Fi APs," in *IEEE Transactions on Vehicular Technology*, pp. 10909–10925, 2019.

[23] Q. Wang, X. Du, Z. Gao, and M. Guizani, "An Optimal Channel Occupation Time Adjustment Method for LBE in Unlicensed Spectrum," in *IEEE Transactions on Vehicular Technology*, pp. 10943–10955, 2019.

[24] J. Xiao, J. Zheng, L. Chu, and Q. Ren, "Performance Modeling and Analysis of the LAA Category-4 LBT Procedure," in *IEEE Transactions on Vehicular Technology*, pp. 10045–10055, 2019.

[25] W. Zhou, J. Sutton, A. Zhang, P. Liu and S. Pan,, "Delay-Guaranteed Admission Control for LAA Coexisting With WiFi," in *IEEE Wireless Communications Letters*, pp. 1048–1051, 2019.
[26] L. B. Jiang and S. C. Liew, "Proportional fairness in wireless plans and ad hoc networks," in *IEEE WCNC*, vol. 3, March 2005, pp. 1551–1556.
[27] L. Li, M. Pal, and Y. R. Yang, "Proportional Fairness in Multi-Rate Wireless LANs," in *IEEE INFOCOM - The 27th Conference on Computer Communications*, April 2008, pp. 1678–1686.
[28] V. A. Siris and G. Stamatakis, "Optimal CWmin Selection for Achieving Proportional Fairness in Multi-Rate 802.11e WLANs: Test-bed Implementation and Evaluation," in *ACM International Workshop on Wireless Network Testbeds, Evaluation, and CHaracterization*, Sep. 2006.
[29] P. Campos, A. Hernández-Solana, and A. Valdovinos-Bardají, "Analysis of Hidden Node Problem in LTE Networks Deployed in Unlicensed Spectrum," in *Computer Networks*, 2020.
[30] A.M. Baswade, T.A. Atif, B.R. Tamma, and A.A. Franklin "LAW: A novel mechanism for addressing hidden terminal problem in LTE-U and Wi-Fi networks," in *IEEE Communications Letters*, 2018.
[31] T.A. Atif, A.M. Baswade, B.R. Tamma, and A.A. Franklin, "A Complete Solution to LTE-U and Wi-Fi HiddenTerminal Problem," in *IEEE Transaction on Cognitive Communications and Networking*, 2019.
[32] A.M. Baswade, T.A. Atif, B.R. Tamma, and A.A. Franklin, "LTE-U and Wi-Fi hidden terminal problem: How serious is it for deployment consideration?," in *International Conference on Communication Systems & Networks (COMSNETS)*, 2018.
[33] F. M. Abinader, E. P. Almeida, F. S. Chaves, A. M. Cavalcante, R. D. Vieira, R. C. Paiva, A. M. Sobrinho, S. Choudhury, E. Tuomaala, K. Doppler, *et al.*, "Enabling the coexistence of LTE and Wi-Fi in unlicensed bands,"*IEEE Communications Magazine*, vol. 52, no. 11, pp. 54–61, 2014.
[34] A. M. Cavalcante, E. Almeida, R. D. Vieira, S. Choudhury, E. Tuomaala, K. Doppler, F. Chaves, R. C. Paiva, and F. Abinader, "Performance evaluation of LTE and Wi-Fi coexistence in unlicensed bands," in *2013 IEEE VTC Spring*, pp. 1–6, 2013.
[35] Y. Jian, C.-F. Shih, B. Krishnaswamy, and R. Sivakumar, "Coexistence of Wi-Fi and LAA: Experimental evaluation, analysis, and insights," in *IEEE ICCW*, pp. 2325–2331, 2015.
[36] Qualcomm, "Qualcomm Research LTE in Unlicensed Spectrum: Harmonious Coexistence With Wi-Fi, Qualcomm Technol. Inc., San Diego, CA, USA, Jun. 2014.
[37] A. Mukherjee, J.-F. Cheng, S. Falahati, L. Falconetti, A. Furuskär, B. Godana, H. Koorapaty, D. Larsson, Y. Yang, *et al.*, "System architecture and coexistence evaluation of licensed-assisted access LTE with IEEE 802.11," in *2015 IEEE ICCW*, pp. 2350–2355, 2015.
[38] P. Chatzimisios, V. Vitsas, and C. Boucouvalas, "Throughput and delay analysis of IEEE 802.11 protocol", in *Proceedings 3rd IEEE International Workshop on System-on-Chip for Real-Time Applications*, 2002.
[39] C. Cano and D. J. Leith, "Unlicensed LTE/Wi-Fi coexistence: Is LBT inherently fairer than CSAT?," in *2016 IEEE ICC*, pp. 1–6, 2016.
[40] C. Cano and D. J. Leith, "Coexistence of Wi-Fi and LTE in unlicensed bands: A proportional fair allocation scheme," in *2015 IEEE ICCW*, pp. 2288–2293, 2015.
[41] 3GPP, "3GPP RAN1 status on LAA and NR-Unlicensed," *IEEE 802.11-18/0542r0*, March 2018.
[42] IEEE 802.11 Coexistence Workshop, July 2019 `http://grouper.ieee.org/groups/802/11/Workshops/2019-July-Coex/workshop.htm`.
[43] R. Kwan, R. Pazhyannur, J. Seymour, V. Chandrasekhar, S. Saunders, D. Bevan, H. Osman, J. Bradford, J. Robson, and K. Konstantinou, "Fair coexistence of licensed assisted access LTE (LAA) and Wi-Fi in unlicensed spectrum," in *2015 7th CEEC*, pp. 13–18, IEEE, 2015.
[44] A. Pratap, R. Singhal, R. Misra, and S.K Das, "Distributed Randomized *k*-Clustering Based PCID Assignment for Ultra-Dense Femto cellular Networks," in *IEEE Transactions on Parallel and Distributed Systems*, pp. 1247–1260, 2018.
[45] Xiph.org, "Derf's Test Media collection," `https://media.xiph.org/video/derf`, accessed May 2020.
[46] M. Iqbal, V. Sathya, N. Norlen, D. Fernandez, M. Ghosh, , A. Ibrahim. and W. Payne, "A Comparison Study of Cellular Deployments in Chicago and Miami Using Apps on Smartphones," in ACM *WINTECH*, March. 2021, pp. 61–68.